Hindawi
Journal of Advanced Transportation
Volume 2022, Article ID 1647306, 28 pages
https://doi.org/10.1155/2022/1647306

Research Article

Collaborative Optimization of Passenger Control Strategy and Train Operation Plan with Variable Formations for a Rail Transit Network

Yonghao Yin,[1] **Jun Chen**,[1] **and Wenrui Zhao**[2]

[1]*Institute of Artificial Intelligence and Robotics (IAIR), Key Laboratory of Traffic Safety on Track of Ministry of Education, School of Traffic and Transportation Engineering, Central South University, Changsha 410075, Hunan, China*
[2]*Dalian Station, China Railway Shenyang Group Co., Ltd., Dalian 116000, Liaoning, China*

Correspondence should be addressed to Jun Chen; cschenjun@csu.edu.cn

Received 30 March 2022; Revised 18 April 2022; Accepted 5 May 2022; Published 13 June 2022

Academic Editor: Xianyu Wu

Copyright © 2022 Yonghao Yin et al. This is an open access article distributed under the Creative Commons Attribution License, which permits unrestricted use, distribution, and reproduction in any medium, provided the original work is properly cited.

We proposed a passenger control strategy and train operation plan collaborative optimization (PCS&TOP) model to schedule the train operation that improves the efficiency of passengers' travel and reduces the cost of train operation for a rail transit network. The model is an integer non linear programming model that aims to minimize the entrance and platform waiting time of passengers and the operation cost of trains. The timetable and variable train formation are integrated optimized, and the turnaround of rolling stock is also considered by constructing the train operation constraints for the model. The coordination of timetables on different lines and the coordination of passenger control strategies at different stations are mentioned by considering the transfer passengers when constructing the passenger control constraints. To solve the model, a multi-operator simulated annealing (MOSA) algorithm that includes three types of execution operators corresponding to three main decision variables is proposed. A numerical case that includes 2 bidirectional crossed lines and a real-world case from China are introduced to test the efficiency of the proposed method, which demonstrates better performance than the single and respective optimization solutions.

1. Introduction

The rail transit system is developing rapidly in recent years, the passenger demand is increasing greatly, and the transport service capacity is insufficient, especially in the central areas of large cities. In the rail transit system, the congestion problem during peak periods and the low train loading rate problem during off-peak periods have been widely noticed by rail transit operators and transportation researchers [1]. How to deal with the oversaturated demand during peak periods and the excessed service during off-peak periods are urgent problems to be solved. The core of that is the mismatch between supply (service capacity from train operation) and demand (travel demand from passengers). The mismatch problem may have a great effect on the competitiveness of rail transit, which is a serious challenge for rail transit operators.

To solve the mismatch problem, there are two main approaches: adjust serving capacity and control passenger demand [2].

The most direct way to satisfy the various demand is to adjust the serving capacity based on the time-varying passenger demand [3]. Demand-driven timetabling increase the serving capacity by dispatching more vehicles during peak hours, which can reduce the passenger waiting time effectively [4]. Meanwhile, the service frequency can be declined during the off-peak hours to reduce operation costs [5]. What's more, to increase the flexibility of train operation, the variable train formation plan is also considered when optimizing the operation plan [6–8]. By doing so, the large formation trains can be used during peak hours to serve more passengers and the small formation trains can be used during off-peak hours to save operation costs. When the double-track line is considered in the research scenario, the

connection of trains at the terminal stations or the restriction of available vehicles should be noticed. With the limited number of rolling stocks, the feasibility of the timetable can be guaranteed [9, 10]. However, due to the limitation of the infrastructure, the improvement in service capacity during peak hours is limited [11], and more demand is induced with increasing supply which may result in the "Downs–Thomson paradox" [12]. Therefore, the mismatch problem cannot be completely solved by just optimizing the train operation plan.

Another way to match supply with demand is to control the passenger demand, especially for the peak periods when the serving capacity reaches its limit. The passenger control strategy with physical barriers (e.g., stockades) is a widely used measure that can provide significant improvements for the congested traffic states [11]. For example, in the Beijing subway (2019), passenger control strategies are applied on more than 90 busy stations (in total 459 stations) during peak hours. A couple of researches focused on the passenger control problem. At the beginning, the scenario is confined to a single station, where the impact on the downstream stations was overlooked [13]. It is noteworthy that the passenger control strategy on different stations should be optimized coordinatively so that the limited serving capacity can be used sufficiently [14]. Therefore, several researchers focus on the coordinative passenger control on multiple stations in the network to minimize passengers' waiting time [15–17].

To further solve the mismatch problem, improve the efficiency of passengers' travel, and decrease the train operation cost, several researchers focus on the joint optimization of the passenger control plan and the schedule of operation. Li et al. [18] proposed a joint optimization model considering the train reschedule and passenger control strategy, and the model is formulated as several quadratic programming problems to be solved efficiently and tested on a metro line numerical case. Liu et al. [19] proposed a timetable and passenger control strategy joint optimization model. The trains' utilization and the number of passengers waiting at platforms are balanced by the model, and tested on a metro line numerical case. Zhang [20] proposed a simulation method to match supply with demand by using a multi-agent dynamic interaction technique. The result showed good performance on matching, but the application scenario is quite small due to the complex simulation process.

From the overview of the recent related research (as shown in Table 1), to the best of our knowledge, there is still no efficient model to solve the mismatch problem by collaborative optimizing the passenger control strategy and the train operation plan with the consideration of variable formations, rolling stock turnaround feasibility, timetable coordination, and passenger control coordination.

Therefore, the motivation of this study is to collaboratively schedule the train operation and plan the passenger control strategy for a rail transit network, in which the efficiency of passengers' travel can be improved and the cost of train operation can be saved. Demand-driven timetable, variable train formation plan, feasible turnaround of rolling stock, coordination of timetables on different lines, and the coordination of passenger control strategies at different stations are considered to construct the passenger control strategy and train operation plan collaborative optimization (PCS&TOP) model. A multi-operator simulated annealing (MOSA) algorithm is introduced to efficiently solve the model. A numerical and a real-world rail transit network case are introduced to test the performance of the proposed method.

The contributions of this study are as follows:

(1) A PCS&TOP model is proposed to collaboratively optimize the passenger control and train operation plan of the rail transit network, which has better performance than the single and respective optimization models. The entrance and platform waiting time of passengers and operation cost of trains are considered as the objective of the model to trade off the efficiency of passengers and the cost of operation.

(2) The variable train formation plan that includes multiple types of formations is considered in the model. By doing so, the large formation trains can be used during peak hours to serve more passengers and the small formation trains can be used during off-peak hours to save operation costs. Meanwhile, when optimizing the train operation plan, the timetable and train formation are integrated optimized, in which the turnaround of rolling stock is considered to improve the feasibility of the optimized operation plan.

(3) When optimizing the passenger control strategy, the coordination of passenger control strategies of different stations in the network is considered to increase the utilization of limited transport capacity. Meanwhile, the coordination of timetables between different lines is mentioned by considering the transfer passengers, which can increase the efficiency of passengers further.

(4) A MOSA algorithm that includes three types of execution operators corresponding to the three main decision variables is proposed to solve the PCS&TOP model. A numerical case and a real-world case are introduced to test the efficiency of the proposed method.

The structure of this article is as follows: Section 2 describes the research scenario, proposes the necessary assumptions, and defines the related parameters. Section 3 introduces the PCS&TOP model that includes the constitution of objective function and constraints. Section 4 proposes the framework of the MOSA algorithm and the three types of execution operators. Section 5 illustrates a numerical case and a real-world case to test the efficiency of the proposed method. Section 6 summarizes the main conclusions of the article.

2. Problem Statement

2.1. Scenario Description. In this study, we engage in collaboratively solving the passenger control problem and train

Table 1: An overview of recent related research.

Authors (year)	Scenario	Problem	Objective	VF	RST	TC	PCC
Mo et al. 2021 [8]	Line	TT & RSP & OS	Min PWT at platform & PTT & TOC	√	√	×	×
Wang et al. 2017 [9]	Line	TT & RSP	Min PWT at platform & TOC	×	√	×	×
Wang et al. 2022 [10]	Network	TT & RSP	Min TOC	×	√	×	×
Meng et al. 2020 [14]	Line	PCS	Min PWT at platform	×	×	×	√
Xu et al. 2019 [15]	Network	PCS	Min PWT at platform	×	×	×	√
Li et al. 2021 [17]	Network	PCS	Min PWT at platform	×	×	×	√
Li et al. 2017 [18]	Line	PCS & TR	Min timetable deviations	×	×	×	√
Liu et al. 2018 [19]	Line	PCS & TT	Min trains' utilization, passenger control intensities, waiting passengers	×	√	×	√
Zhang 2021 [20]	Line	PCS & TT	Max matching supply with demand	×	×	×	√
This study	Network	PCS & TOP	Min PWT at entrance and platform, & TOC	√	√	√	√

TT: train timetable; RSP: rolling stock plan; OS: operation strategy; PCS: passenger control strategy; TR: train reschedule; TOP: train operation plan; Max: maximum; Min: minimum; PWT: passenger waiting time; PTT: passenger travel time; TOC: train operation cost; VF: variable formations; RST: rolling stock turnaround; TC: timetable coordination; PCC: passenger control coordination.

operation planning problem in a rail transit network. The integration of timetabling and train formation planning and the coordination of network passenger control strategy are all considered to construct the optimization model; the scenario and related variables are defined as follows:

We focus on a rail transit network with several lines that cross but do not overlap in spatial. As shown in Figure 1, each line is bidirectional, and vehicles are independently operating on each line. The lines are denoted as $l \in \Gamma$, and the indexes are different if the directions of them are different even on the same line. Only passengers can transfer from one line to another at transfer stations, while trains are not.

The stations are denoted as $i \in \Theta_l$ from the origin station to the terminal station. Specifically, Θ_l can be classified as original stations set Θ_O, terminal stations set Θ_D, and transfer stations set Θ_T. To distinguish the same transfer station on different lines, the stations are denoted as $i, i', i'', i''' \in \Theta_T$, respectively.

The train $k \in \Phi_l$ stops at each station, crossing and overtaking are banned at any place. The formation of trains is a variable that includes several types $m \in \Omega$ with different rolling stocks TR^m. The trains can and only can turnover, couple, and decouple at the terminal station on each line, and the number of available rolling stock is considered to guarantee the feasibility of the optimized operation plan.

Passenger demand is known in the planning stage which is obtained by some prediction methods based on the historical passenger demand from the automatic fare collection (AFC) system. The passenger demand on each station is time-varying, and the values of them are counted by each time slice. The time slices $t \in \Pi$ are separated from the total time horizon with a fixed time interval. As the time slice being small enough (1 minute in this study), the variation of passenger demand can be described. The time-varying dynamic passenger demand can be explained as the number of arrival passengers $PAS^i(t)$, passenger alighting ratio $PRA^i(t)$, and transferring ratio $PRT^{i,i'}(t)$.

To control the passengers during congested periods, the passenger control strategy is classified as several levels $u \in \Psi$ and several time slices Δt in spatial and temporal, respectively. By doing so, the passenger control strategy is more

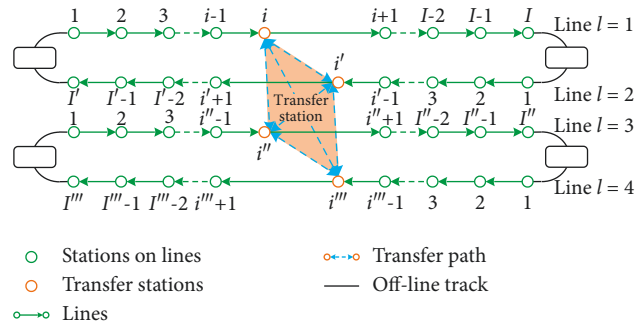

Figure 1: Illustration of a rail transit network.

executable. RA_u represents the specific flow control ratio corresponding to the related level u, which is the value of controlled passengers divided by waiting passengers. The study time slice is so small that the strategy cannot be timely adjusted following the optimized solution in reality, and the complexity of the model may greatly increase. Therefore, the passenger control strategy is defined as a large granularity with a four-time slice ($\Delta t = 4t$). Based on that, the number of passengers in each place is defined and the relationship between them is restricted by the passenger control constraints that will be discussed in Section 3.

In summary, the collaborative optimization problem is formally stated as follows: based on the known parameters, the PCS&TOP model aims to minimize the passenger waiting time at the platform ptf, passenger waiting time at the entrance pte, and train operation cost toc. By doing so, a train operation plan with variable formation plan, available rolling stock, and demand-driven timetables on different lines and a collaborative network passenger control strategy can be obtained.

2.2. Assumption and Parameter Definition. Four assumptions are proposed to simplify the research scenario and describe the model.

(1) The order of passengers at any place during the same time slice in the rail transit system is viewed as random. Based on that, we just focus on the number

of passengers on each place during each time, and the destination can be ignored. The passenger distribution has been counted and only has a small deviation [21].

(2) The influence of crowded passengers is ignored, so the trains' running time in each section and dwelling time in each station are fixed on each line. All trains stop at each station, crossing and overtaking are banned at any position. The number of rolling stocks and the formation type are limited [22].

(3) To guarantee the passenger control strategy is more operable and reduce the complexity of the optimization model, the strength of passenger control strategy is restricted to several levels, and the granularity of passenger control strategy is restricted as Δt time duration. Specifically, the strategies are the same at the same level during Δt time slices. With the increase of the levels' number and decreasing the duration of time slices, the strategy is more accurate, but the efficiency of optimization process and the difficulty of strategy execution are increasing [23]. Besides, the number of separated levels and the granularity can be changed to fit the application of the specific scenario.

(4) The transfer time $TT^{i,i'}$ is viewed as a fixed value based on the average walk speed that can greatly simplify the model but only has a small influence [24].

The indexes, sets, parameters, and variables used in this article are introduced in Table 2, and the decision variables are separately explained in detail as follows:

There are three decision variables and seven intermediate variables which are further explained in detail as follows:

(1) Train Departure Time Variable. As shown in the following expression, the train departure time $td_k^i(t)$ represents whether the train departs from the station at the current time.

$$td_k^i(t) = \begin{cases} 1, & \text{if train } k \text{ departs from station } i \text{ at time } t \text{ on line } l, \\ 0, & \text{otherwise,} \end{cases} \quad \text{for } \forall i \in \Theta_l,\ \forall t \in \Pi,\ \forall k \in \Phi_l,\ \forall l \in \Gamma. \tag{1}$$

(2) Train Formation Variable. As shown in the following expression , the train formation ty_k^m represents whether the train k used the formation m.

$$ty_k^m = \begin{cases} 1, & \text{if train } k \text{ used formation } m, \\ 0, & \text{otherwise,} \end{cases} \quad \text{for } \forall m \in \Omega,\ \forall k \in \Phi_l,\ \forall l \in \Gamma. \tag{2}$$

(3) Passenger Control Level Variable. As shown in (3), the passenger control level $pc_u^i(t)$ represents whether the strength of passenger control is u level at the station i in time t. As shown in Figure 2, the passenger control strength is divided into several levels (11 levels in this study) corresponding to different control strengths. RA_u is the alternative flow control ratio, which is the value of the controlled passengers divided by the waiting passengers. $\sum_{u\in\Psi} pc_u^i(t) \times Ra_u$ is the executive flow control ratio at the station i in time t. Level 1 is a strategy without control (all passengers can enter the station), and level 11 is a strategy with total control (no passengers can enter the station). Meanwhile, the strategy can also be separated as more levels or fewer levels that depend on the intricacy of the passenger control. By doing so, the number of the passenger control decision variable and the complexity of the model is greatly decreased so that the model can be solved efficiently (Jiang et al., 2018). Therefore, $pc_u^i(t)$ is a Boolean variable.

$$pc_u^i(t) = \begin{cases} 1, & \text{if passenger flow control level is } u \text{ at station } i \text{ at time } t, \\ 0, & \text{otherwise,} \end{cases} \quad \text{for } \forall u \in \Psi,\ \forall i \in \Theta_l,\ \forall l \in \Gamma,\ \forall t \in \Pi. \tag{3}$$

(4) Number of Passengers in Different Space Variables. The number of passengers in different space variables including $pw^i(t)$, $pe^i(t)$, $pf^i(t)$, $pb_k^i(t)$, $pa_k^i(t)$, $pl_k^i(t)$, and $pt_k^i(t)$ are nonnegative integer intermediate variables. They depend on the optimized timetable, and the relationships of them are also have an influence on the value of them; the specific calculation process will be introduced in Section 3.

$$pw^i(t), pe^i(t), pf^i(t) \in \mathrm{N}, \quad \text{for } \forall i \in \Theta_l, \forall l \in \Gamma, \forall t \in \Pi,$$
$$pb_k^i(t), pa_k^i(t), pl_k^i(t), pt_k^i(t) \in \mathrm{N}, \quad \text{for } \forall i \in \Theta_l, \forall k \in \Phi_l, \forall l \in \Gamma, \forall t \in \Pi. \tag{4}$$

3. Passenger Control Strategy and Train Operation Plan Collaborative Optimization Model

The PCS&TOP model that includes the objective function and related constraints are introduced in this section.

3.1. Objective Function of the PCS&TOP Model. Three aspects that include passenger waiting time at the platform ptf, passenger waiting time at the entrance pte, and train operation cost toc are considered in the objective function of the PCS&TOP model that are shown as follows:

$$\mathbf{min}\ obj = \alpha_1 \times ptf + \alpha_2 \times pte + \alpha_3 \times toc. \tag{5}$$

The passenger travel cost depends on the efficiency of passengers, and the delay in travel is one of the most direct indicators to explain passengers' efficiency. In a crowded rail transit system, due to the oversaturated passenger demand and limited train loading capacity, passengers may be remaining at the platform which leads to a delay for passengers called left-behind delay. To analyze the passenger

Table 2: The explanation of sets, indexes, parameters, and variables.

	Indexes and sets
Π	Set of time $\Pi = \{t \mid t = 1, 2, \ldots, T\}$, t is time index
Γ	Set of lines, line index $l \in \Gamma$
Ω	Set of train formations, in which train formation index $m \in \Omega$
Ψ	Set of passenger control level, in which flow control level index $u \in \Psi$
Θ_l	Set of stations on line l, in which station index $i, i', i'', i''' \in \Theta_l$. Θ_l can be classified as original stations set: Θ_O, terminal stations set: Θ_D, transfer stations set: Θ_T
Φ_l	Set of trains on line l, in which train index $k, k' \in \Phi_l$
	Parameters and variables
obj	Objective function value
ptf	Total passenger waiting time at platform
pte	Total passenger waiting time at entrance due to control strategy
toc	Total train operation cost
TRT^l	Train operation time of a train with a unit formation on line l
TR^m	Number of rolling stocks for train formation m
TS	Time slice, which is set as 1 minute in this study
TW_l^i	Train dwell time at station i on line l
TR_l^i	Train running time from station i to station $i+1$ on line l
TTR_l^i	Train turnover time at terminal station i on line l
$TH_{\min}$	Minimum headway between two successive trains
$TH_{\max}$	Maximum headway between two successive trains
$NK_{l,\max}$	Maximum number of train services in total time on line l
$PAS^i(t)$	Number of arrived passengers on station i at time t
$PRA^i(t)$	Ratio of alighting passengers on station i at time t
$PRT^{i,i'}(t)$	Ratio of transferring passengers from station i to i' at time t, $i, i' \in \Theta_T$
Cap^m	Service capacity for train formation m
RA_u	Alternative passenger control ratio at level u
Δt	Passenger control time slice
$TT^{i,i'}$	Transfer time from station i to station i'
$\alpha_1, \alpha_2, \alpha_3$	Weight parameters of objective function
$pw^i(t)$	Number of waiting passengers at entrance on station i at time t
$pe^i(t)$	Number of entering passengers on station i at time t
$pf^i(t)$	Number of waiting passengers at platform on station i at time t
$pb_k^i(t)$	Number of boarding passengers to train k on station i at time t
$pa_k^i(t)$	Number of alighting passengers from train k on station i at time t
$pl_k^i(t)$	Number of loading passengers in train k on station i at time t
$pt_k^i(t)$	Number of transfer passengers in train k on station i at time t
	Decision variables
$td_k^i(t)$	Train departure time variable
ty_k^m	Train formation variable
$pc_u^i(t)$	Passenger control level variable

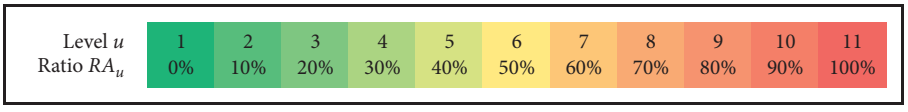

Figure 2: The diagram of passenger control level.

left-behind delay, the passenger waiting time at the platform ptf is calculated. As shown in the following equation, the number of passengers at the platform $pf^i(t)$ of each station on each line at each time slice is counted and multiplied by the length of a time slice TS (1 minute in this study) to calculate ptf.

$$ptf = TS \times \sum_{l \in \Gamma} \sum_{i \in \Theta_l} \sum_{t \in \Pi} pf^i(t). \tag{6}$$

The passenger left-behind delay and the crowding condition at the platform can be eased by carrying out the passenger control strategy at the entrance. However, the passenger control may lead to to another delay for passengers called passenger control delay. To analyze the passenger control delay, the passenger waiting time at the entrance pte is calculated. As shown in the following equation, the number of waiting passengers at the entrance $pw^i(t)$ of each station on each line at each time is counted and multiplied by a time slice TS to calculate pte.

$$pte = TS \times \sum_{l \in \Gamma} \sum_{i \in \Theta_l} \sum_{t \in \Pi} pw^i(t). \tag{7}$$

Train operation cost is proportional to the operation time of a unit formation and the number of used formations

[25]. The used formations are related to the selected train type ty_k^m of service k and the formations TR^m of the train type m. The operation time of a unit formation is represented by TRT^l that is different on different lines. Therefore, the total train operation time can be calculated as follows:

$$toc = \sum_{l\in\Gamma}\sum_{k\in\Phi_l}\sum_{m\in\Omega} TRT^l \times TR^m \times ty_k^m. \tag{8}$$

3.2. Constraints of the PCS&TOP Model. The constraints of the PCS&TOP model that include train operation constraints, passenger control constraints, and variable range constraints are introduced as follows:

3.2.1. Train Operation Constraints. To guarantee the train operation safety and provide efficient service, the timetable-related decision variables are restricted. To guarantee the optimized timetable is feasible, the number of available formations and the usage of rolling stock are considered, and the formation-related decision variables are restricted.

(1) Train Departure Time Constraints. Train departure time is one of the most important decision variables in this study, and the departure times of a train at successive stations have a relationship. Specifically, as shown in the following expression, the departure time of a train on the current station $td_k^i(t)$ is related to the departure times of the train on the previous station $td_k^{i-1}(t)$, the train running time between the stations TR_l^i, and the train dwelling time on the current station TW_l^i:

$$\sum_{t\in\Pi} td_k^i\left(t + TR_l^i + TW_l^i\right) \times t = \sum_{t\in\Pi} td_k^{i-1}(t) \times t,$$
$$\text{for } \forall i \in \Theta_l/\{\Theta_O\}, \forall k \in \Phi_l, \forall l \in \Gamma, \tag{9}$$

(2) Headway of Operation Train Constraints. To guarantee the train operation safety, the minimum headways of trains are restricted. As shown in (10), the number of train services has at most one during a minimum safety headway time horizon. Meanwhile, to guarantee the train service efficiency, the maximum headway of trains should be restricted. As shown in (11), the number of train services has at least one during a maximum headway time horizon.

$$\sum_{k\in\Phi_l}\left(\sum_{t=t'}^{t'+TH_{\min}-1} td_k^i(t) \times \sum_{m\in\Omega} ty_k^m\right) \le 1, \quad \text{for } \forall i \in \Theta_l, \forall l \in \Gamma, \forall t' \in [1, T - TH_{\min} + 1], \tag{10}$$

$$\sum_{k\in\Phi_l}\left(\sum_{t=t'}^{t'+TH_{\max}} td_{k,n}^i(t) \times \sum_{m\in\Omega} ty_k^m\right) \ge 1, \quad \text{for } \forall i \in \Theta_l, \forall l \in \Gamma, \forall t' \in [1, T - TH_{\max}]. \tag{11}$$

(3) Order of Operation Train Constraints. As the train departure time $td_k^i(t)$ and train formation ty_k^m are Boolean decision variables, the order of trains should be restricted. Specifically, as shown in (12), when the train k and train k' are all used, the equation will work. Then, the departure time of the former train should be earlier than the departure time of the later train.

$$\begin{aligned}(k - k') \times &\left(\sum_{t\in\Pi} td_k^i(t) \times t - \sum_{t'\in\Pi} td_{k'}^i(t') \times t'\right)\\ &+ \left(\sum_{m\in\Omega} ty_k^m + \sum_{m\in\Omega} ty_k^m - 2\right) \times M \ge 0,\\ &\text{for } \forall k, k' \in \Phi_l, \forall i \in \Theta_l, \forall l \in \Gamma.\end{aligned} \tag{12}$$

(4) Maximum Number of Operating Train Constraints. (13) restricts the type of train formation to that at most one. If the train is operated, one formation is selected; otherwise, no formation will be selected. (14) restricts the total number of train services on line l in the study time horizon.

$$\sum_{m\in\Omega} ty_k^m \le 1, \text{ for } \forall k \in \Phi_l, \forall l \in \Gamma. \tag{13}$$

$$\sum_{k\in\Phi_l}\sum_{m\in\Omega} ty_k^m \le NT_{l,\max}, \text{ for } \forall l \in \Gamma. \tag{14}$$

(5) Rolling Stock Turnaround Constraints. To guarantee the optimized timetable and formation plan are feasible, the turnaround of rolling stock and the available number of vehicles are considered. (15) is to guarantee the number of remaining vehicles is not less than 0. Specifically, the number of remaining vehicles on a line is related to the total number of vehicles RS_l (first part in the constraint), the number of departed vehicles (second part in the constraint), and the number of arrival vehicles (third part in the constraint).

$$RS_l - \sum_{k\in\Phi_l}\sum_{t'\subseteq[1,t]} td_k^i\left(t' - TW_l^i\right)\times\sum_{m\in\Omega} ty_k^m + \sum_{k'\in\Phi_{l'}}\sum_{t'\subseteq[1,t]} td_{k'}^{i'}\left(t' + TTR_{l'}^{i'}\right)\times\sum_{m'\in\Omega} ty_{k'}^{m'} \geq 0,$$
$$\text{for } \forall i \in \Theta_l \cap \Theta_O, \forall i' \in \Theta_{l'} \cap \Theta_D, \forall l, l' \in \Gamma, \forall t \in \left[1 + TW_l^i, T - TTR_{l'}^{i'} + 1\right]. \tag{15}$$

3.2.2. Passenger Control Constraints. The process of passengers' travel in the rail transit system can be broken up into several steps: arriving at the entrance, entering the entrance, arriving at the platform, waiting on the platform, boarding the train, taking the train, alighting the train, transferring to the platform of another line (if the transfer is needed, then following the previous step: arriving at the platform and continue), and exiting the station. The number of passengers in each place has a close relationship, so the process can be explained by just a few variables to reduce the complexity of the model. Therefore, we introduce the variables one by one based on the process of passengers' travel, and then some intermediate variables are reduced and the constraints are simplified. Finally, the variables $pw^i(t)$, $pf^i(t)$, and $pa_k^i(t)$ are replaced, and all constraints are explained by the variables $pe^i(t)$, $pb_k^i(t)$, $pl_k^i(t)$, and $pt_k^i(t)$.

(1) The Number of Waiting Passengers at the Entrance. Due to the passenger control strategy, passengers may be controlled at the entrance and waiting at the entrance. Therefore, the number of passengers waiting at the entrance is related to the number of arrival passengers $PAS^i(t)$ and the passenger control level $pc_u^i(t)$ (as shown in (16)). As time goes on, it is also related to the number of passengers waiting at the entrance during previous time slice $pw^i(t-1)$ (as shown in (17)).

$$pw^i(t) = PAS^i(t)\times\sum_{u\in\Psi} pc_u^i(t)\times RA_u, \quad \text{for } \forall i \in \Theta_l, \forall l \in \Gamma, \forall t = 1, \tag{16}$$

$$pw^i(t) = \left(pw^i(t-1) + PAS^i(t)\right)\times\sum_{u\in\Psi} pc_u^i(t)\times RA_u, \quad \text{for } \forall i \in \Theta_l, \forall l \in \Gamma, \forall t \in \Pi\backslash\{1\}. \tag{17}$$

Then, accumulating the (18) in the successive time slice to replace $pw^i(t-1)$, the relationship between flow control level $pc_u^i(t)$ and number of passenger waiting at the entrance $pw^i(t)$ can be constructed as (22).

$$pw^i(t) = \sum_{t'\subseteq[1,t]}\left[PAS^i(t')\times\prod_{t''\subseteq[t',t]}\left(\sum_{u\in\Psi} pc_u^i(t'')\times RA_u\right)\right],$$
$$\text{for } \forall i \in \Theta_l, \forall l \in \Gamma, \forall t \in \Pi. \tag{18}$$

Therefore, in the objective function, the passenger waiting time at the entrance pte can be explained by the passenger control level $pc_u^i(t)$. Set equation (19) into equation (8) to obtain equation (20).

$$pte = TS\times\sum_{l\in\Gamma}\sum_{i\in\Theta_l}\sum_{t\in\Pi}\sum_{t'\subseteq[1,t]}\left[PAS^i(t')\times\prod_{t''\subseteq[t',t]}\left(\sum_{u\in\Psi} pc_u^i(t'')\times RA_u\right)\right]. \tag{19}$$

(2) The Number of Entering Passengers. As shown in (20) and (21), $pe^i(t)$ is the number of passengers entering the station i at the entrance during time slice t, which is related to the number of arrival passengers $PAS^i(t)$ and the number of waiting passengers at the entrance $pw^i(t)$. Meanwhile, it is also related to the number of passengers waiting at the entrance during the previous time slice $pw^i(t-1)$ as time goes on.

$$pe^i(t) = PAS^i(t) - pw^i(t), \quad \text{for } \forall i \in \Theta_l, \forall l \in \Gamma, \forall t = 1, \tag{20}$$

$$pe^i(t) = pw^i(t-1) + PAS^i(t) - pw^i(t), \quad \text{for } \forall i \in \Theta_l, \forall l \in \Gamma, \forall t \in \Pi\backslash\{1\}. \tag{21}$$

To replace $pw^i(t)$ and $pw^i(t-1)$, set (18) into (20) to obtain (22), set (18) into (21) to obtain (23).

$$pe^i(t) = PAS^i(t)\times\left(1 - \sum_{u\in\Psi} pc_u^i(t)\times RA_u\right), \quad \text{for } \forall i \in \Theta_l, \forall l \in \Gamma, \forall t = 1, \tag{22}$$

$$pe^i(t) = \sum_{t'\subseteq[1,t-1]}\left[PAS^i(t')\times\prod_{t''\subseteq[t',t]}\left(\sum_{u\in\Psi} pc_u^i(t'')\times RA_u\right)\right] + PAS^i(t) - \sum_{t'\subseteq[1,t]}\left[PAS^i(t')\times\prod_{t''\subseteq[t',t]}\left(\sum_{u\in\Psi} pc_u^i(t'')\times RA_u\right)\right],$$
$$\text{for } \forall i \in \Theta_l, \forall l \in \Gamma, \forall t \in \Pi\backslash\{1\}. \tag{23}$$

Simplify equation (23), and (24) can be obtained as follows:

$$
\begin{aligned}
pe^i(t) = & \sum_{t' \subseteq [1,t-1]} \left[PAS^i(t') \times \prod_{t'' \subseteq [t',t]} \left(\sum_{u \in \Psi} pc_u^i(t'') \times RA_u \right) \right] + PAS^i(t) \\
& - \left\{ \sum_{t' \subseteq [1,t-1]} \left[PAS^i(t') \times \prod_{t'' \subseteq [t',t-1]} \left(\sum_{u \in \Psi} pc_u^i(t'') \times RA_u \right) \right] + PAS^i(t) \right\} \times \left(\sum_{u \in \Psi} pc_u^i(t) \times RA_u \right) \\
& = \left\{ \sum_{t' \subseteq [1,t-1]} \left[PAS^i(t') \times \prod_{t'' \subseteq [t',t-1]} \left(\sum_{u \in \Psi} pc_u^i(t'') \times RA_u \right) \right] + PAS^i(t) \right\} \times \left(1 - \sum_{u \in \Psi} pc_u^i(t) \times RA_u \right) \\
& \text{for } \forall i \in \Theta_l, \forall l \in \Gamma, \forall t \in \Pi \backslash \{1\}.
\end{aligned} \tag{24}
$$

(3) The Number of Passengers on the Platform. After the passengers enter the station, they will wait the trains on the platform. As shown in (25) and (26), the number of passengers on the platform $pf^i(t)$ is related to the number of passengers entering the station $pe^i(t)$, the number of transfer passengers $pt_k^i(t)$, and the number of passengers boarding the train $pb_k^i(t)$. As time goes on, it is also related to the number of passengers on the platform at the previous time slice $pf^i(t-1)$.

$$
\begin{aligned}
pf^i(t) = & pe^i(t) + \sum_{k \in \Phi_l} \left(pt_k^i(t) - pb_k^i(t) \right), \\
& \text{for } \forall i \in \Theta_l, \forall l \in \Gamma, \forall t = 1,
\end{aligned} \tag{25}
$$

$$
\begin{aligned}
pf^i(t) = & pf^i(t-1) + pe^i(t) + \sum_{k \in \Phi_l} \left(pt_k^i(t) - pb_k^i(t) \right), \\
& \text{for } \forall i \in \Theta_l, \forall l \in \Gamma, \forall t \in \Pi \backslash \{1\}.
\end{aligned} \tag{26}
$$

Accumulate (26) in successive time slice to replace $pf^i(t-1)$:

$$
\begin{aligned}
pf^i(t) = & \sum_{t' \subseteq [1,t]} \left[pe^i(t') + \sum_{k \in \Phi_l} \left(pt_k^i(t') - pb_k^i(t') \right) \right], \\
& \text{for } \forall i \in \Theta_l, \forall l \in \Gamma, \forall t \in \Pi.
\end{aligned} \tag{27}
$$

In the objective function, the passenger waiting time at the platform ptf can be explained by $pe^i(t)$, $pt_k^i(t)$, and $pb_k^i(t)$. Set (27) into (6) to obtain

$$
ptf = TS \times \sum_{l \in \Gamma} \sum_{i \in \Theta_l} \sum_{t \in \Pi} \sum_{t' \subseteq [1,t]} \left[pe^i(t') + \sum_{k \in \Phi_l} \left(pt_k^i(t') - pb_k^i(t') \right) \right]. \tag{28}
$$

(4) The Number of Passengers Boarding the Train. The passengers will board the train when the trains arrive at the station. The number of passengers boarding the train $pb_k^i(t)$ should not be over the number of passengers waiting at the platform during the current time slice. Therefore, as shown in (29) and (30), the number of boarding passengers is related to the entered passengers $pe^i(t)$ and transferred passengers during the current time slice $pt_k^i(t)$, and the waiting passengers on the platform during the previous time slice $pf^i(t-1)$, and whether the train arrives. Only when the train arrives $(td_k^i(t) \times \sum_{m \in \Omega} ty_k^m = 1)$, the number of boarding passengers is possibly larger than 0; otherwise, no passengers board the train and the value must be 0.

$$
\begin{aligned}
pb_k^i(t) \le & \left(pe^i(t) + pt_k^i(t) \right) \times td_k^i(t) \times \sum_{m \in \Omega} ty_k^m, \\
& \text{for } \forall k \in \Phi_l, \forall i \in \Theta_l, \forall l \in \Gamma, \forall t = 1.
\end{aligned} \tag{29}
$$

$$
\begin{aligned}
pb_k^i(t) \le & \left(pf^i(t-1) + pe^i(t) + pt_k^i(t) \right) \times td_k^i(t) \times \sum_{m \in \Omega} ty_k^m, \\
& \text{for } \forall k \in \Phi_l, \forall i \in \Theta_l, \forall l \in \Gamma, \forall t \in \Pi \backslash \{1\}.
\end{aligned} \tag{30}
$$

To replace $pf^i(t)$, set (27) into (30) to obtain

$$
\begin{aligned}
pb_k^i(t) \le & \left\{ \sum_{t' \subseteq [1,t-1]} \left[pe^i(t') + \sum_{k \in \Phi_l} \left(pt_k^i(t') - pb_k^i(t') \right) \right] \right. \\
& \left. + pe^i(t) + pt_k^i(t) \right\} \times td_k^i(t) \times \sum_{m \in \Omega} ty_k^m, \\
& \text{for } \forall k \in \Phi_l, \forall i \in \Theta_l, \forall l \in \Gamma, \forall t \in \Pi \backslash \{1\}.
\end{aligned} \tag{31}
$$

Simplify (31) and combine with (29)to get the following expression:

$$
\begin{aligned}
pb_k^i(t) \le & \left[\sum_{t' \subseteq [1,t]} \left(pe^i(t') + \sum_{k \in \Phi_l} pt_k^i(t') \right) \right. \\
& \left. + \sum_{t' \subseteq [1,t-1]} \sum_{k \in \Phi_l} pb_k^i(t') \right] \times td_k^i(t) \times \sum_{m \in \Omega} ty_k^m, \\
& \text{for } \forall k \in \Phi_l, \forall i \in \Theta_l, \forall l \in \Gamma, \forall t \in \Pi.
\end{aligned} \tag{32}
$$

(5) The Number of Passengers Alighting the Train. As shown in (33) and (34), the number of alighting passengers $pa_k^i(t)$ is related to the number of passengers on the train $pl_k^{i-1}(t-1)$, and the passenger alighting ratio $PRA^i(t)$, and whether the train arrives. As there are no passengers who will alight at the first station or during the first time slice, $pa_k^i(t)$ is 0. Only when the train arrives $(td_k^i(t) \times \sum_{m \in \Omega} ty_k^m = 1)$, the number of alighting passengers is possible larger than 0; otherwise, no passengers alight the train and the value must be 0. Meanwhile, the passenger alighting

ratio $PRA^i(t)$ is a time-varying parameter that is calculated by the historical passenger distribution and widely used in previous research [21].

$$pa_k^i(t) = 0, \quad \text{for } (\forall i \in \Theta_O, \forall t \in \Pi) \cup (\forall i = \Theta_l, \forall t = 1), \quad \forall k \in \Phi_l, \forall l \in \Gamma, \tag{33}$$

$$pa_k^i(t) = pl_k^{i-1}(t-1) \times PRA^i(t) \times td_k^i(t) \times \sum_{m \in \Omega} ty_k^m, \quad \text{for } \forall i = \Theta_l \backslash \{\Theta_O\}, \forall k \in \Phi_l, \forall l \in \Gamma, \forall t \in \Pi \backslash \{1\}. \tag{34}$$

(6) The Number of Passengers Transferring between Different Lines. The number of transferring passengers $pt_k^i(t)$ is related to the alighting passengers, the transferring ratio $PRT^{i',i}(t)$, and whether the train arrives. As shown in (35), there are no passengers who will transfer at intermediate stations during any time slice. Only when the train arrives $(td_k^i(t) \times \sum_{m \in \Omega} ty_k^m = 1)$, the number of transferring passengers is possible larger than 0; otherwise, no passengers transfer to other trains and the value must be 0. Meanwhile, the passenger transferring ratio $PRT^{i',i}(t)$ is also a time-varying parameter and depends on the historical passenger distribution [21].

$$pt_k^i(t) = 0, \quad \text{for } \forall k \in \Phi_l, \forall i \in \Theta_l \backslash \{\Theta_T\}, \forall l \in \Gamma, \forall t \in \Pi. \tag{35}$$

$$pt_k^i\left(t + TS^{i',i}\right) = \sum_{i' \in \Theta_T / \{i\}} \left(pa_k^{i'}(t) \times PRT^{i',i}(t)\right) \times td_k^i(t) \times \sum_{m \in \Omega} ty_k^m, \quad \text{for } \forall k \in \Phi_l, \forall i, i' \in \Theta_T, \forall l \in \Gamma, \forall t \in \left[1, T - TS^{i',i}\right]. \tag{36}$$

Set (34) into (36), and $pa_k^i(t)$ can be replaced and obtained as follows:

$$pt_k^i\left(t + TS^{i',i}\right) = \sum_{i' \in \Theta_T / \{i\}} \left(pl_k^{i-1}(t-1) \times PRA^i(t) \times PRT^{i',i}(t)\right) \times td_k^i(t) \times \sum_{m \in \Omega} ty_k^m, \quad \text{for } \forall k \in \Phi_l, \forall i, i' \in \Theta_T, \forall l \in \Gamma, \forall t \in \left[1, T - TS^{i',i}\right]. \tag{37}$$

(7) The Number of Passengers on the Train. The number of passengers on the train $pl_k^i(t)$ is related to the boarding passengers $pb_k^i(t)$, loading passengers during the previous time slice $pl_k^i(t-1)$, alighting passengers $pa_k^i(t)$, and whether the train arrives. The scenarios during the first time slice or not and on the first station or not are separately discussed, and the equations (38)–(40) are constructed. Only when the train arrives $(td_k^i(t) \times \sum_{m \in \Omega} ty_k^m = 1)$, the number of passengers on the train $pl_k^i(t)$ is changed; otherwise, it equals the loading passengers during the previous time slice $pl_k^i(t-1)$.

$$pl_k^i(t) = pb_k^i(t) \times td_k^i(t) \times \sum_{m \in \Omega} ty_k^m, \quad \text{for } \forall i = \Theta_O, \forall k \in \Phi_l, \forall l \in \Gamma, \forall t = 1, \tag{38}$$

$$pl_k^i(t) = pl_k^i(t-1) \times \left(1 - td_k^i(t) \times \sum_{m \in \Omega} ty_k^m\right) + pb_k^i(t) \times td_k^i(t) \times \sum_{m \in \Omega} ty_k^m, \quad \text{for } \forall i = \Theta_O, \forall k \in \Phi_l, \forall l \in \Gamma, \forall t \in \Pi \backslash \{1\}, \tag{39}$$

$$pl_k^i(t) = pl_k^i(t-1) \times \left(1 - td_k^i(t) \times \sum_{m \in \Omega} ty_k^m\right) + \left(pl_k^{i-1}(t-1) + pb_k^i(t) - pa_k^i(t)\right) \times td_k^i(t) \times \sum_{m \in \Omega} ty_k^m \quad \text{for } \forall i = \Theta_l \backslash \{\Theta_O\}, \forall k \in \Phi_l, \forall l \in \Gamma, \forall t \in \Pi \backslash \{1\}. \tag{40}$$

Set (34) into (40), and $pa_k^i(t)$ can be replaced and obtained as follows:

$$\begin{aligned} pl_k^i(t) = pl_k^i(t-1) \times \left(1 - td_k^i(t) \times \sum_{m\in\Omega} ty_k^m\right) \\ + \left[pl_k^{i-1}(t-1) \times \left(1 - PRA^i(t)\right) + pb_k^i(t)\right] \\ \times td_k^i(t) \times \sum_{m\in\Omega} ty_k^m, \\ \text{for } \forall i = \Theta_l \backslash \{\Theta_O\}, \forall k \in \Phi_l, \forall l \in \Gamma, \forall t \in \Pi \backslash \{1\}. \end{aligned} \tag{41}$$

(8) The Train Capacity Constraints. Due to the limitation of train loading capacity, the number of passengers on the train has an upper bound. As shown in (42), it depends on the train formation and the capacity of different formations.

$$pl_k^i(t) \le \sum_{m\in\Omega} ty_k^m \times Cap^m, \quad \text{for } \forall i = \Theta_l, \forall k \in \Phi_l, \forall l \in \Gamma, \forall t \in \Pi. \tag{42}$$

(9) The Passenger Control Level Constraints. As shown in (43), the strategy at each station during each time slice selects one and only one level to execute the passenger control measure.

$$\sum_{u\in\Psi} pc_u^i(t) = 1, \quad \text{for } \forall i = \Theta_l, \forall l \in \Gamma, \forall t \in \Pi. \tag{43}$$

(10) The Passenger Control Strategy's Granularity Constraints. The total study time horizon is separated as many time slices with a 1-minute length, and the time slice is so small that the flow control strategy cannot be timely adjusted following the optimized solution in reality. Meanwhile, such a small granularity strategy may greatly increase the complexity of the model. Therefore, we proposed (44) to increase the granularity of the passenger control strategy that guarantees the strategies are the same during Δt time slices.

$$\begin{aligned} pc_u^i(t + \Delta t) - pc_u^i(t) = 0, \quad \text{for } \forall u \in \Psi, \forall i = \Theta_l, \\ \forall l \in \Gamma, \forall \Delta t \subseteq [1, TH_{\min} - 1], \forall t \in \Pi, \forall t / TH_{\min} \in Z^+. \end{aligned} \tag{44}$$

3.2.3. Variable Range Constraints. As intermediate variables $pw^i(t)$, $pf^i(t)$, and $pa_k^i(t)$ are replaced by other variables, the model includes three Boolean decision variables $td_k^i(t)$, ty_k^m, and $pc_u^i(t)$ and four integer intermediate variables $pe^i(t)$, $pb_k^i(t)$, $pl_k^i(t)$, and $pt_k^i(t)$. The range of each variable is shown in equations (45)–(48).

$$\begin{aligned} td_k^i(t) = 0 \text{ or } 1, \\ \text{for } \forall i \in \Theta_l, \forall k \in \Phi_l, \forall l \in \Gamma, \forall t \in \Pi, \end{aligned} \tag{45}$$

$$\begin{aligned} ty_k^m = 0 \text{ or } 1, \\ \text{for } \forall m \in \Omega, \forall k \in \Phi_l, \forall l \in \Gamma, \end{aligned} \tag{46}$$

$$\begin{aligned} pc_u^i(t) = 0 \text{ or } 1, \\ \text{for } \forall u \in \Psi, \forall i \in \Theta_l, \forall l \in \Gamma, \forall t \in \Pi, \end{aligned} \tag{47}$$

$$\begin{aligned} pe^i(t), pb_k^i(t), pl_k^i(t), pt_k^i(t) \in N, \\ \text{for} \forall i \in \Theta_l, \forall k \in \Phi_l, \forall l \in \Gamma, \forall t \in \Pi. \end{aligned} \tag{48}$$

In summary, the PCS&TOP model is proposed as follows:

$$\text{PCS\&TOP model} \begin{cases} \textbf{Objective function}: (5), (8), (19), (28), \\ \textbf{Constitutions}:, \\ \textbf{Train operation}\ (9)-(15), \\ \textbf{Passenger flow control}, \\ (22), (24), (32), (35), (37)-(39), (41)-(44), \\ \textbf{Variable range}\ (45)-(48). \end{cases} \tag{49}$$

3.3. Complexity Analysis of the PCS&TOP Model. The complexity of the PCS&TOP model depends on the scale of decision variables. The scale of decision variables includes the number of time slices $|\Pi|$, the number of lines $|\Gamma|$, the number of stations $|\Theta_l|$, the number of trains $|\Phi_l|$, the number of train formations $|\Omega|$, and the number of passenger control levels $|\Psi|$. To count conveniently, the scenarios on different lines are the same, and the numbers of constraints in the model are listed in Table 3. Most of the constraints are related to the number of time slices $|\Pi|$; the number of constraints is so large that may greatly affect the solving efficiency even though the model can be linearized and solved by commercial solvers. Besides, the optimality of the result is not necessary and the optimized result is what we pursued because there will be deviations in the manual execution process in reality. Therefore, a heuristic algorithm is proposed to solve the PCS&TOP model in the next section to trade off the solving efficiency and optimality.

4. Multi-Operator Simulated Annealing Algorithm to Solve the PCS&TOP Model

As the proposed PCS&TOP model is an integer non linear programming model that includes many non linear constraints, an intelligent heuristic algorithm is proposed to solve the model.

Table 3: The number of constraints in the PCS&TOP model.

Constraints	Number of constraints
Constraint (9)	$(\lvert\Theta_l\rvert - 1) \times \lvert\Phi_l\rvert \times \lvert\Gamma\rvert$
Constraints (10) and (11)	$\lvert\Theta_l\rvert \times \lvert\Gamma\rvert \times 2 \times \lvert\Pi\rvert$
Constraint (12)	$\lvert\Theta_l\rvert \times (\lvert\Phi_l\rvert - 1) \times \lvert\Phi_l\rvert \times \lvert\Gamma\rvert$
Constraints (13) and (14)	$(\lvert\Phi_l\rvert + 1) \times \lvert\Gamma\rvert$
Constraint (15)	$4 \times \lvert\Theta_l\rvert \times \lvert\Pi\rvert$
Constraints (22) and (24)	$\lvert\Theta_l\rvert \times \lvert\Gamma\rvert \times \lvert\Pi\rvert$
Constraint (32)	$\lvert\Theta_l\rvert \times \lvert\Phi_l\rvert \times \lvert\Gamma\rvert \times \lvert\Pi\rvert$
Constraints (35) and (37)	$\lvert\Theta_l\rvert \times \lvert\Phi_l\rvert \times \lvert\Gamma\rvert \times \lvert\Pi\rvert$
Constraints (38), (39) and (41)	$\lvert\Theta_l\rvert \times \lvert\Phi_l\rvert \times \lvert\Gamma\rvert \times \lvert\Pi\rvert$
Constraints (42)–(44)	$\lvert\Theta_l\rvert \times \lvert\Gamma\rvert \times \lvert\Psi\rvert \times \lvert\Pi\rvert / TH_{\min}$
Constraints (45)–(48)	$[(4 \times \lvert\Phi_l\rvert + \lvert\Psi\rvert + 1) \times \lvert\Theta_l\rvert \times \lvert\Pi\rvert + \lvert\Omega\rvert \times \lvert\Phi_l\rvert] \times \lvert\Gamma\rvert$

The optimization process of passenger control strategy and train operation plan needs to adjust slightly because the optimized strategies are similar, and so do the timetables. Meanwhile, we should also avoid falling into the local optimality with several similar solutions. The architecture of the simulated annealing (SA) algorithm can respond to solving the problems because it has the local search strategy and the random accepted suboptimal solution strategy [26]. To be suitable for the PCS&TOP model, a multi-operator simulated annealing (MOSA) algorithm is proposed, which includes three types of execution operators corresponding to the three main decision variables $td_k^i(t)$, ty_k^m, and $pc_u^i(t)$.

4.1. Algorithm Framework. Based on the architecture of the SA algorithm, the framework of the MOSA algorithm is constructed, and the pseudocode of the MOSA algorithm is shown in Algorithm 1. The algorithm-related parameters and the suggested value of them are listed in Appendix A.

In step 1, the algorithm is initialized by setting the initial value of the algorithm-related parameters, namely iteration times $iter$, initial temperature τ_{iter}, execution times $o_{l,m}$, scores $\mu_{l,m}$, and weights $\theta_{l,m}$.

In step 2, an initial feasible solution s_{init} that includes the train timetable, formation plan, and passenger control strategy is randomly generated, and the initial result obj_{init} is calculated by (5), (8), (19), (28). Then, set the best solution s_{best} and iteration solution s_{iter} as the initial solution s_{init}.

In step 3, first, a line l is selected randomly to adjust; based on the roulette wheel mechanism with weights $\theta_{l,m}$, an operator m is selected to adjust the solution (the specific operator adjustment process will be introduced in the next section); the execution times $\rho_{l,m}$ are calculated based on the current iteration times. Second, operator m ($\rho_{l,m}$ times) is executed to adjust the current solution s_{iter}; the current iteration result obj_{iter} is calculated by (28). Third, compared with the best result, the better result will be accepted as the best result, and the worse result will also be accepted as the current result with a probability. Fourth, the algorithm parameters that include iteration times $iter$, initial temperature τ_{iter}, execution times $o_{l,m}$, scores $\mu_{l,m}$, and weights $\theta_{l,m}$ will be updated based on the above process. Specifically, execution times $o_{l,m}$, scores $\mu_{l,m}$, and weights $\theta_{l,m}$ will be reset as the initial value per φ iterations to avoid the same operator being selected too many times that trapped in the local search. Then, the current temperature τ_{iter} will reheat to the start temperature τ_{start}, and the algorithm parameters will be reset when the current temperature τ_{iter} is smaller than the end temperature τ_{end} and the reheat times γ is smaller than the maximum reheat times $\gamma_{\max}$. Finally, the optimal process will be stopped and jumped to step 4 when the iteration times $iter$ is larger than the maximum iteration times $iter_{\max}$ or the reheat times γ is larger than the maximum reheat times $\gamma_{\max}$.

In step 4, the best result obj_{best} and the best solution s_{best} are returned that includes the train timetable, formation plan, and passenger control strategy.

4.2. Execution Operators. As the model includes three types of decision variables, three types of execution operators are proposed that can adjust the solution and guarantee the feasibility of the solution [27]. Specifically, the execution operators are classified as train timetable (TT) operators, train formation (TF) operators, and passenger control (PC) operators. The specific selection and update process of the execution operators is shown in Figure 3, which corresponds to Steps 3.1–3.4 in the MOSA algorithm.

4.2.1. Train Timetable Operators. TT operators are proposed to adjust the train timetable (decision variable $td_k^i(t)$), which include four destroy operators that change the timetable based on different features and two repair operators that make the adjusted solution feasible based on the constraints of the model.

(i) TT_D_1: randomly increase train headway

Randomly select a train: k;

The train's timetable moves backward 1-time slice: $td_k^i(t+1) \leftarrow td_k^i(t)$;

Execute train timetable repair operator TT_R_1.

(ii) TT_D_2: randomly decrease train headway

Randomly select a train: k;

The train's timetable moves forward 1-time slice: $td_k^i(t-1) \leftarrow td_k^i(t)$;

Execute train timetable repair operator TT_R_2.

(iii) TT_D_3: increase headway on low loading rate train

Input:
Passenger demand parameters: $PAS^i(t)$, $PRA^i(t)$, $PRT^{i,i'}(t)$
Passenger control parameters: RA_u, Δt
Train operation parameters: TRT^l, TR^m, TS, TW_l^i, TR_l^i, $TH_{\min}$, $TH_{\max}$, $NK_{l,\max}$, Cap^m, $TT^{i,i'}$
Other model parameters: $\alpha_1, \alpha_2, \alpha_3$
Other algorithm parameters: τ_{start}, τ_{end}, ϕ, $\gamma_{\max}$, $iter_{\max}^{\text{per}}$, $iter_{\max}$, φ, λ_1, λ_2.
Output:
Best solution s_{best}; best objective value obj_{best}.
(1) Step 1: Initialize
(2) $iter \leftarrow 1$, $\tau_{iter} \leftarrow \tau_{start}$, $\gamma_{iter} \leftarrow 0$, $o_{l,m} \leftarrow 0$, $\mu_{l,m} \leftarrow 0$, $\theta_{l,m} \leftarrow 1$, for $l \in \Gamma, m \in \text{M}$;
(3) Step 2: Calculate initial result
(4) Randomly generate an initial solution s_{init} and make it feasible
(5) Calculate the initial result obj_{init} by equations (5), (8), (19), (28)
(6) Set $s_{\text{best}} \leftarrow s_{iter} \leftarrow s_{\text{init}}$, $obj_{\text{best}} \leftarrow obj_{iter} \leftarrow obj_{\text{init}}$
(7) Step 3: Optimize passenger control strategy and train operation plan
(8) while ($\gamma_{iter} \le \gamma_{\max}$) do
(9) while ($\tau_{iter} \ge \tau_{\text{end}}$) do
(10) Set $s_{\text{iter}}' \leftarrow s_{\text{iter}}$, $obj_{\text{iter}}' \leftarrow obj_{\text{iter}}$;
(11) Step 3.1: Select operators
(12) Randomly select a line l;
(13) Based on roulette wheel mechanism with weights $\theta_{l,m}$, select an operator m;
(14) Calculate the execution times $\rho_{l,m}$ based on iteration times;
(15) Step 3.2: Perform operators
(16) Execute operator m on s_{iter} by $\rho_{l,m}$ times;
(17) Calculate the current result obj_{iter} by (5), (8), (19), (28);
(18) Step 3.3: Update best solution
(19) Accept better result or accept suboptimal result with a probability, and store
(20) best solution $s_{best} \leftarrow s_{iter}$, $obj_{\text{best}} \leftarrow obj_{iter}$;
(21) Step 3.4: Update algorithm parameters
(22) Update iteration times $iter \leftarrow iter + 1$, and temperature $\tau_{iter} \leftarrow \tau_{iter} \times \phi$;
(23) Update execution times $o_{l,m}$, scores $\mu_{l,m}$, and weights $\theta_{l,m}$;
(24) Reset $o_{l,m} \leftarrow 0$, $\mu_{l,m} \leftarrow 0$, $\theta_{l,m} \leftarrow 1$ for $l \in \Gamma, m \in \text{M}$ per φ iterations;
(25) Step 3.5: Decide stopping conditions
(26) If $\tau_{iter} < \tau_{\text{end}}$, jump to Step 3.6; else, continue;
(27) If $iter > iter_{\max}$, jump to Step 4; else continue;
(28) end while
(29) Step 3.6: Reheat process
(30) Reheat temperature $\tau_{iter} \leftarrow \tau_{\text{start}}$, $\gamma_{iter} \leftarrow \gamma_{iter} + 1$;
(31) Reset algorithm parameters $o_{l,m} \leftarrow 0$, $\mu_{l,m} \leftarrow 0$, $\theta_{l,m} \leftarrow 1$ for $l \in \Gamma, m \in \text{M}$.
(32) If $\gamma_{iter} > \gamma_{\max}$, jump to Step 4; else continue;
(33) end while
(34) Step 4: Return best result
(35) Return s_{best}, obj_{best}.

Algorithm 1: MOSA algorithm.

Calculate train loading passengers, and build a low loading rate train set: $\Phi_{\text{low},l}$;

Select a train from the low loading rate trains set: k;

The train's timetable moves backward 1-time slice: $td_k^i(t+1) \leftarrow td_k^i(t)$;

Execute train timetable repair operator TT_R_1.

(iv) TT_D_4: decrease headway on high loading rate train

Calculate train loading passengers, consider the adjustable headway of trains, and build a high loading rate trains set: $\Phi_{\text{high},l}$;

Select a train from the low loading rate train set: k;

The train's timetable moves forward 1-time slice: $td_k^i(t-1) \leftarrow td_k^i(t)$;

Execute train timetable repair operator TT_R_2.

(v) TT_R_1: repair headway increasing broken

If headway constraint (11) of trains $k-1$ and k is broken, roll back;

If headway constraint (10) of trains k and $k+1$ is broken, the timetable of all following trains (except for last train K_l) move backward 1-time slice $td_{k'}^i(t+1) \leftarrow td_{k'}^i(t)\,(\forall k' \subseteq [k+1, K_l - 1])$;

If headway constraint (10) of trains $K_l - 1$ and K_l is broken, cancel train $K_l - 1$;

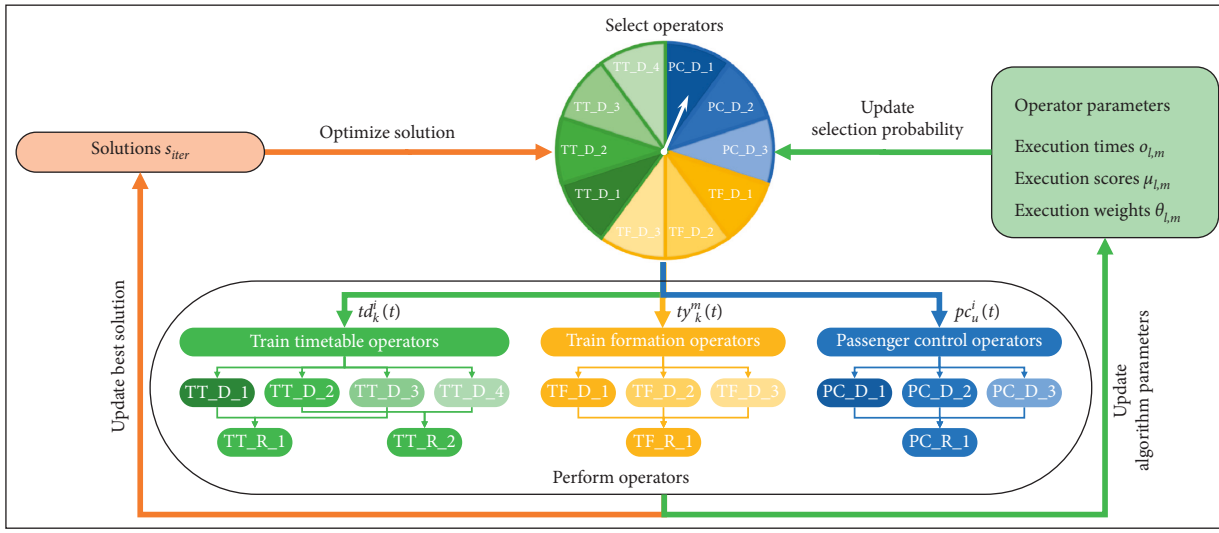

Figure 3: The selection and update process of execution operators.

If rolling stock turnaround constraints (14) and (15) are broken, roll back.

(vi) TT_R_2: repair headway decreasing broken

If headway constraint (10) of trains $k-1$ and k is broken, roll back;

If headway constraint (11) of trains k and $k+1$ is broken, the timetable of all following trains (except for last train K_l) move forward 1-time slice $td_{k'}^i(t-1) \leftarrow td_{k'}^i(t)\,(\forall k' \subseteq [k+1, K_l - 1])$;

If headway constraint (11) of trains $K_l - 1$ and K_l is broken, add a new train with a random formation in the middle of the two trains.

If rolling stock turnaround constraints (14) and (15) are broken, roll back.

4.2.2. Train Formation Operators. TF operators are proposed to adjust the train formation (decision variable ty_k^m), which includes three destroy operators that change the formation based on different features and a repair operator that makes the adjusted solution feasible based on the constraints of the model.

(i) TF_D_1: randomly change train formation

Randomly select a train: k;

Randomly change the train's formation: $ty_{k'}^m \leftarrow ty_k^m$;

Execute train formation repair operator TF_R_1.

(ii) TF_D_2: decrease formation on low loading rate train

Calculate train loading passengers, consider the adjustable formation of trains, and build a low loading rate trains set: $\Phi_{\text{low},l}$;

Select a train from the low loading rate train set: k;

Decrease the train's formation: $ty_k^{m-1} \leftarrow ty_k^m$;

Execute train formation repair operator TF_R_1.

(iii) TF_D_3: increase formation on high loading rate train

Calculate train loading passengers, consider the adjustable formation of trains, and build a high loading rate trains set: $\Phi_{\text{high},l}$;

Select a train from the high loading rate train set: k;

Increase the train's formation: $ty_k^{m+1} \leftarrow ty_k^m$;

Execute train formation repair operator TF_R_1.

(iv) TF_R_1: repair formation changing broken

If rolling stock turnaround constraints (14) and (15) are broken, roll back.

4.2.3. Passenger Control Operators. PC operators are proposed to adjust the passenger control strategy (decision variable $pc_u^i(t)$), which includes three destroy operators that change the passenger control level based on different features and a repair operator that makes the adjusted solution feasible based on the constraints of the model.

(i) PC_D_1: randomly change passenger control level

Randomly select a time slice: Δt;

Randomly increase/decrease a control level: $pc_u^i(t) \leftarrow pc_u^i(t) \pm 1$ for $t \subseteq [1, \Delta t]$;

Execute passenger control strategy repair operator PC_R_1.

(ii) PC_D_2: increase passenger control level during time slice with a high left-behind rate

Calculate the number of passengers on the platform $pf^i(t)$, consider the adjustable strategy level, and build a high left-behind rate time slices set: $\Pi_{\text{left-behind}}$;

Select a time slice from the high left-behind rate time slices set: Δt;

Increase a passenger control level: $pc_u^i(t) \leftarrow pc_u^i(t) + 1$ for $t \subseteq [1, \Delta t]$;

Execute passenger control strategy repair operator PC_R_1.

(iii) PC_D_3: decrease passenger control level during time slice with a high control rate

Calculate the number of passengers on the platform $pf^i(t)$, consider the adjustable strategy level, and build a high control rate time slices set: $\Pi_{control}$;

Select a time slice from the high control rate time slices set: Δt;

Decrease a passenger control level: $pc_u^i(t) \leftarrow pc_u^i(t) - 1$ for $t \subseteq [1, \Delta t]$;

Execute passenger control strategy repair operator PC_R_1.

(iv) PC_R_1: repair passenger control level changing broken

If passenger control constraints (42)–(44) are broken, roll back.

5. Case Study

A numerical case and a real-world case are introduced to test the efficiency of the proposed the PCS&TOP model and the MOSA algorithm in this section.

5.1. Numerical Case Study

5.1.1. Case Description. As shown in Figure 4, a numerical case that includes 2 bidirectional crossed lines is illustrated. Every line has 5 stations that include an origin station (Station 1), a terminal station (Station 5), and a transfer station (Station 3). The related parameters that include the train operation parameters and passenger demand are listed in Appendix B. During the 60-minute study time horizon, we pursue the optimal train operation plan and passenger control strategy plan by calculating the PCS&TOP model and MOSA algorithm.

The computation process is performed on a Windows 11 (64-bit) workstation with an AMD Ryzen 7–4800U CPU and 16 GB RAM. The MOSA algorithm is programmed in MATLAB 2021a.

5.1.2. Result Analysis. To avoid the randomness of the MOSA algorithm, we test the experiment 50 times with the same parameters ($\alpha_1 = 1$, $\alpha_2 = 100$, $\alpha_3 = 0.7$). The average computation time is 260.47 seconds (4.34 minutes). The values of the objective function in the 50 experiments are shown in Figure 5, the minimum result is 125,282 obtained 26 times. Three other different solutions are obtained and all results are within a 0.5% gap compared with the minimum one. Therefore, the MOSA algorithm performs well in terms of convergence.

In the minimum result, the passenger waiting time at the platform is 33,748 minutes, the passenger waiting time at the entrance is 7,048 minutes, and the train operation cost is 866 corresponding to 62 train service that includes 34 1-unit formation trains and 28 2-unit formation trains. The specific results are shown in the next section and compared with the results in other conditions.

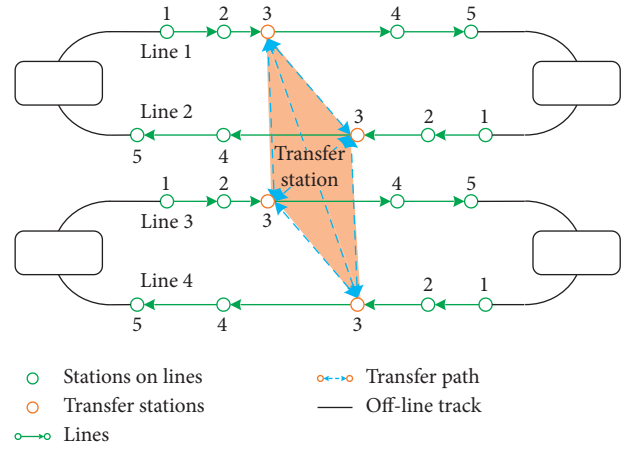

Figure 4: Illustration of the numerical case rail transit network.

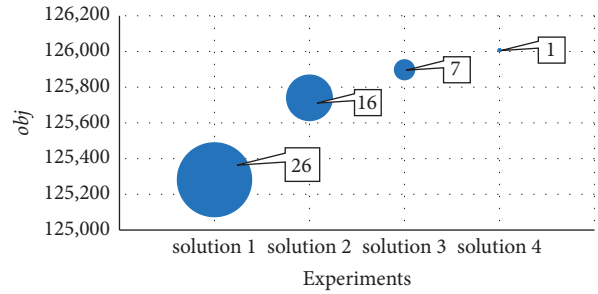

Figure 5: The results of 50 experiments with the same parameters.

Table 4: Comparison of the objective function and each part in different results.

Results	*obj*	*ptf*	*pte*	*toc*	Trains
Origin	171,232	43,232	0	1,280	64 (0, 64)
PCS	169,668	36,152	7,880	1,280	64 (0, 64)
TOP	125,520	38,920	0	866	62 (34, 28)
PCS&TOP	125,282	33,748	7,048	866	62 (34, 28)

Notes: tr (tr_1, tr_2) in "Trains"—tr represents the total number of trains, and tr_1 and tr_2 represent the number of trains in type 1 and type 2, respectively.

5.1.3. Result Comparison. To show the efficiency of the proposed model and algorithm, the optimized result is compared with the results in different conditions.

The origin solution is proposed as the original scenario. The timetables operating with minimum headways on each line are the same, and all trains are 2-unit formation. Meanwhile, there are no passenger control strategies at any station at any time. The PCS result is the solution that optimizes the passenger control strategy with the original train operation plan. The TOP result is the solution that optimized the train operation plan without any passenger control strategy. The PCS&TOP result is the collaborative

Figure 6: The platform waiting time of passengers in different solutions.

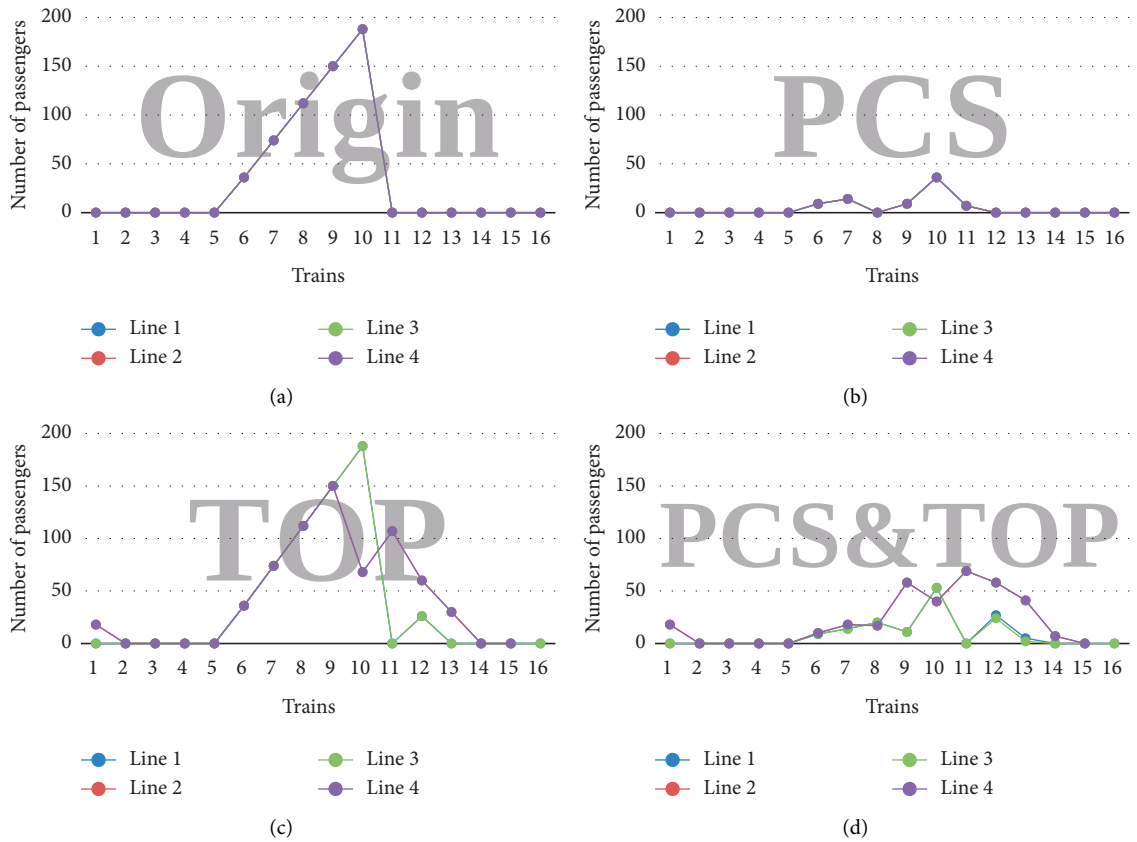

Figure 7: The number of left-behind passengers in different solutions. (a) Origin solution; (b) PCS solution; (c) TOP solution; and (d) PCS&TOP solution.

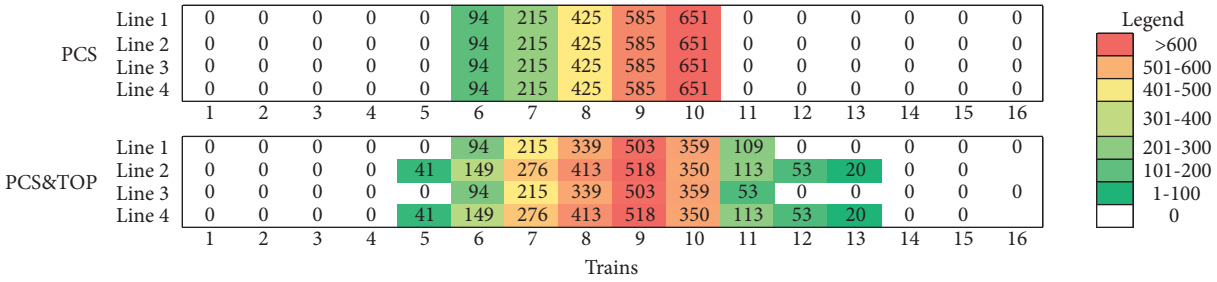

Figure 8: The entrance waiting time of passengers in different solutions.

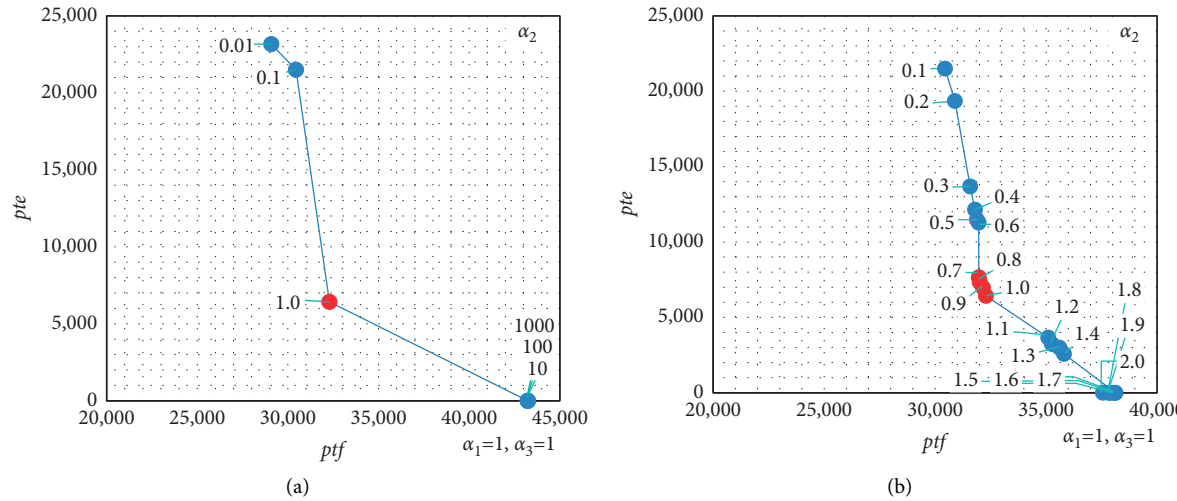

Figure 9: Pareto curve of results with different values of α_2. (a) Range from 0.01 to 1000; and (b) Range from 0.1 to 2.0.

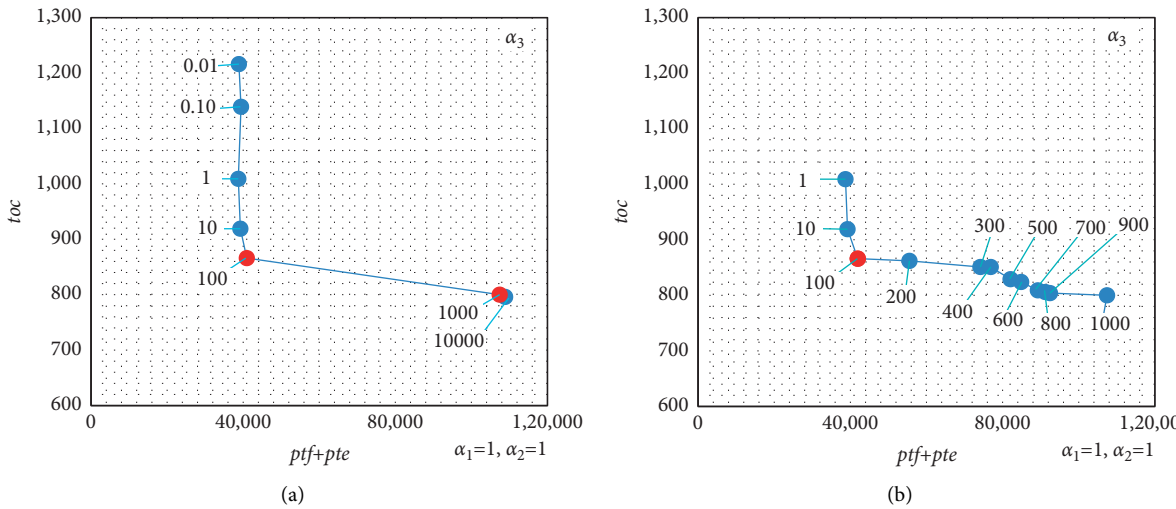

Figure 10: Pareto curve of results with different values of α_3. (a) Range from 0.01 to 10000; (b) range from 1 to 1000.

optimization solution of passenger control strategy and train operation plan by the proposed model and algorithm.

The values of the objective function and each part are compared and shown in Table 4. Compared with the origin result, the passenger waiting time at the platform is decreased in PCS, because the passengers are controlled at the entrance; the train operation cost is decreased in TOP because the timetables of different lines and train formation are integrated optimized; both are decreased in PCS&TOP. Whereas, the passenger waiting time at the entrance is

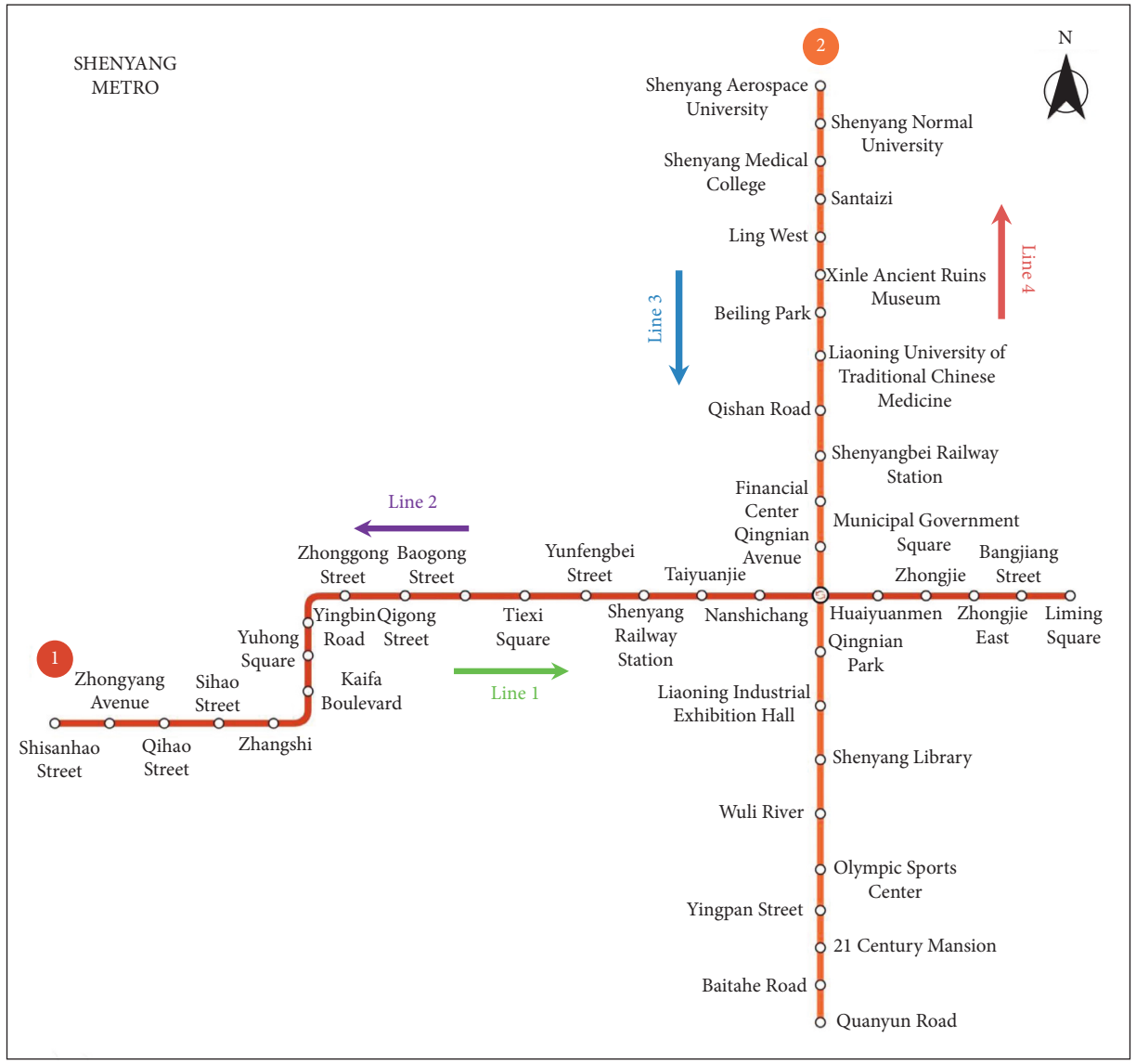

Figure 11: Illustration of Shenyang Metro network.

increasing in PCS and PCS&TOP. Therefore, the proposed model and algorithm can collaboratively optimize the passenger control strategy and train operation plan.

The platform waiting time of passengers ptf in each train on each line in each solution is shown in Figure 6. The number of passengers is larger, the color on the bar is nearer the red; the number is smaller, the color on the bar is nearer the green; if there are no passengers, the color is white. We find that the total platform waiting time on each train decreased during peak hours (trains 6–11) in PCS&TOP even though it used fewer trains.

The number of left-behind passengers on each line after the trains depart from the station in different solutions is shown in Figure 7. We find that, compared with the solution without passenger control (origin solution and TOP solution), fewer passengers are left behind at the platform in the solution with passenger control (PCS solution and PCS&TOP solution), which shows the benefits of the passenger control strategy. There still have passengers left behind at the platform, because the excessive passenger control strategy may lead to extra delays at the entrance. Meanwhile, the passenger control strategy is discretized as several levels corresponding to several control rates, and the specific control level is selected at each station.

As the passenger control strategy is not considered in the origin and TOP solutions, the entrance waiting time of passengers in the two solutions are 0. The entrance waiting time of passengers in the PCS and PCS&TOP solutions is shown in Figure 8. Compared with the PCS solution, the peak value of entrance passenger waiting time is decreased and the range of them is increased in the PCS&TOP

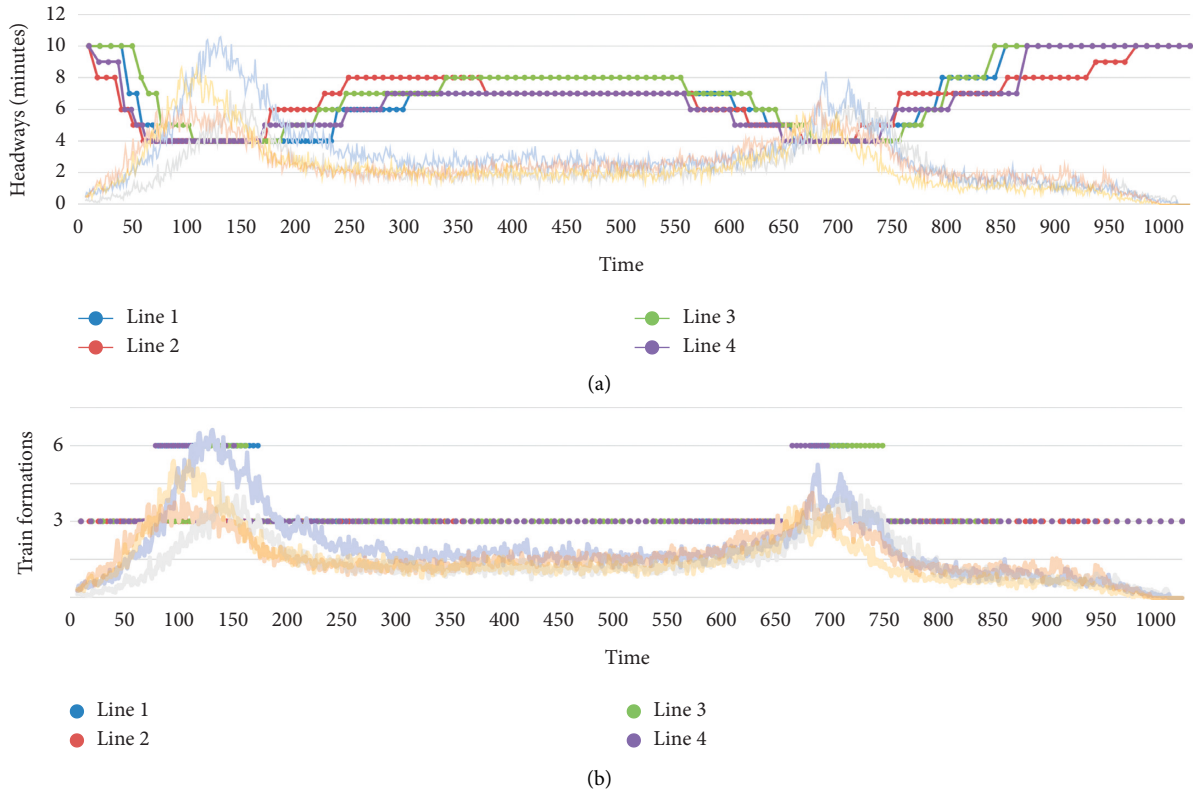

FIGURE 12: Train operation plan and passenger distribution of 4 lines. (a) Headway of trains at origin stations on each line and (b) the formation of trains on each line.

solution, which implies that the passengers are controlled with weaker strength and wider time horizon.

In summary, the proposed model and algorithm can collaboratively optimize the passenger control strategy and train operation plan to reduce the train operation cost and increase the efficiency of passengers.

5.1.4. Sensitive Analysis of the Model's Parameters. (1) Weight Parameter of Passenger Entrance Waiting Time α_2. As the passenger entrance waiting time is directly related to the passenger platform waiting time (if the train operation plan is fixed) that all depends on the passenger control level (as shown in Equations (18), (23), and (28)), the weights of ptf and pte should be discussed to analyze their relationship.

We set the value of α_1 (weight of ptf) and α_3 (weight of toc) as 1, and test the values of α_2 (weight of pte) in a range as wide as possible. Each set of parameters is tested 10 times and selected as the minimum one. Then, the values [0.01, 0.1, 1.0, 10, 100, 1000] are selected and shown in Figure 9(a), the Pareto curve of α_2 is constructed. We find that the result almost no longer changes when $\alpha_2 \leq 0.1$ or $\alpha_2 \geq 10$, which represents the range of α_2 can be obtained. Meanwhile, the α_2 is sensitive near the value 1.0, so the values of α_2 in [0.1, 2.0] with a 0.1 step length are also tested to describe the Pareto curve accurately and shown in Figure 9(b). We find that ptf is reduced a few but may lead to a large increase on pte when the value of α_2 in [0.1, 0.6]. The variation of ptf and pte is nearly similar when the value of α_2 in [1.0, 1.5], and the result almost no longer changes when $\alpha_2 \geq 1.5$. When the value of α_2 in [0.7, 1.0], the results are relatively stabilized and guarantee the control of oversaturated passengers.

In summary, the passenger control strategy depends on the value of α_2, and the operators can adopt different strategies by selecting different values. [0.7, 1.0] is selected as the range of α_2 to optimize the passenger control strategy in this study, because it is the inflection point on the Pareto curve. Specifically, during that range, the oversaturated passengers can be controlled and may not lead to much unnecessary delay. [1.0, 1.5] can be selected if the operators do not focus on the congestion of passengers on the platform. [0.1, 0.6] can be selected if the operators greatly focus on the safety of passengers on the platform, but it may lead to unnecessary delays for passengers.

(2) Weight Parameter of Train Operation Cost α_3. The efficiency of passengers (ptf and pte) is inversely proportional to the train operation cost (toc), so the weights of toc should be discussed to analyze their relationship.

We set the value of α_1 (weight of ptf) and α_2 (weight of pte) as 1, and test the values of α_3 (weight of toc) in a range as wide as possible. Each set of parameters is tested 10 times and selected as the minimum one. Then, the values [0.01, 0.1, 1.0, 10, 100, 1000, 10000] are selected and shown in

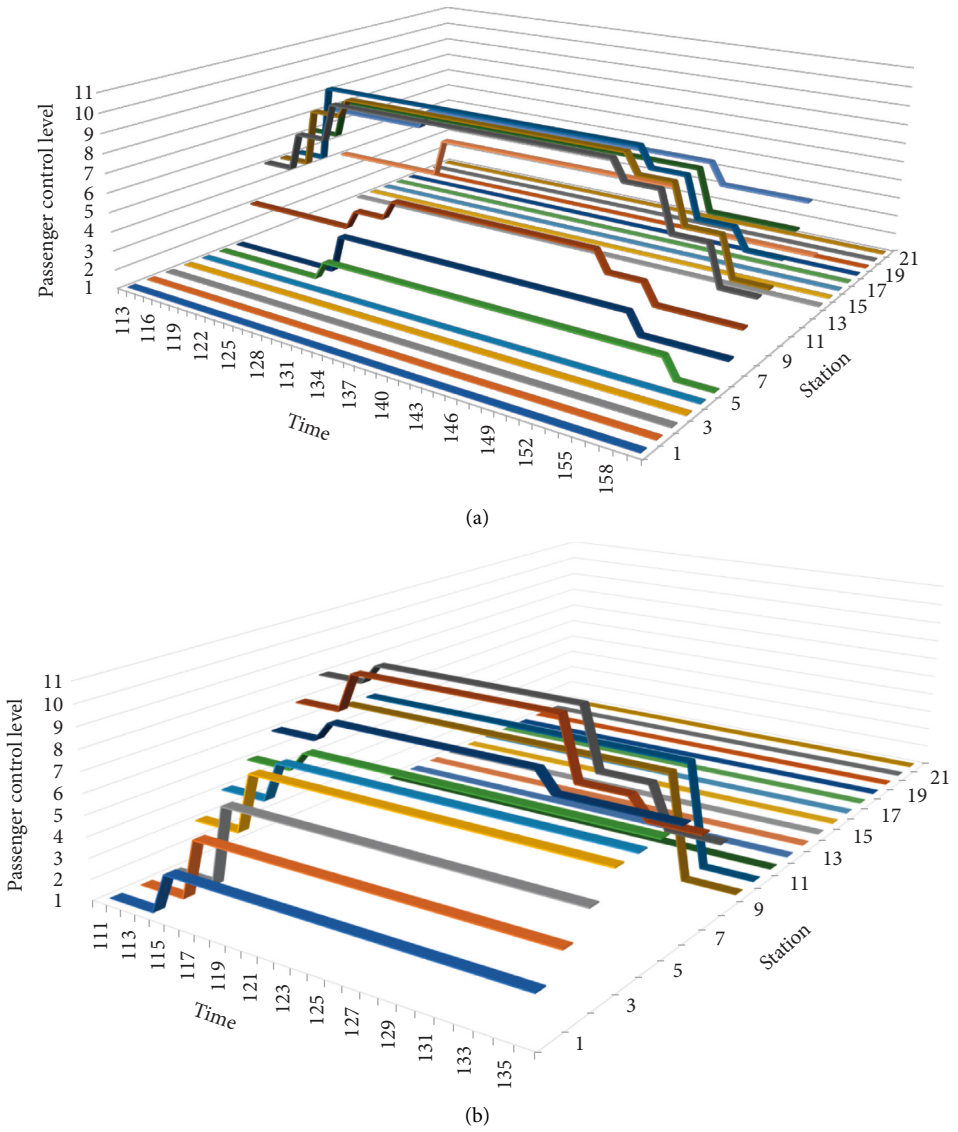

Figure 13: Passenger control strategy of each line. (a) Passenger control strategy of Line 1 and (b) passenger control strategy of Line 4.

Figure 10(a), the Pareto curve of α_3 is constructed. The α_3 is sensitive near the value 100, so the values of α_3 in [100, 1000] with a 100 step length are tested to describe the Pareto curve accurately (Figure 10(b)). We find that the passenger delay (*ptf* and *pte*) is reduced a lot that only needs a few increase on *toc* when the value of α_3 in [100, 1000]; the result almost no longer changes when $\alpha_3 \geq 1000$; the passenger delay (*ptf* and *pte*) is reduced a few but may lead to a large increase on *toc* when the value of α_3 in [0.01, 100].

In summary, the train operation cost depends on the value of α_3. 100 is selected as the value of α_3 to optimize the passenger control strategy in this study because it is the inflection point on the Pareto curve. In the range of [100, 1000], the passenger delay can be reduced a lot, but only leads to a few increases on train operation cost when the value of α_3 is reducing. Meanwhile, the different strategies that are optimized with different values of the weight can be adopted by operators in different scenarios.

5.2. Real-World Case Study

5.2.1. Case Description. A real-world large-scale case from Shenyang Metro (2016) in China is proposed to test the performance of the PCS&TOP model and MOSA algorithm. Two bidirectional lines in Shenyang Metro are considered and the illustration of them is shown in Figure 11.

The two independent operation lines are from east to west (line 1) and from south to north (line 2), and crossed at the transfer station (Qingnian Avenue Station). Only the passengers can transfer at the transfer station while trains cannot crossover the line. Line 1 has 22 stations and includes an up-direction line (from Shisanhao Street station to Liming Square station) denoted as Line 1 and a down-direction line (from Liming Square station to Shisanhao Street station) denoted as Line 2. Line 2 has 22 stations and includes an up-direction line (from Quanyun Road station to Shenyang Aerospace University station) denoted as Line 3 and a down-direction line (from Shenyang Aerospace

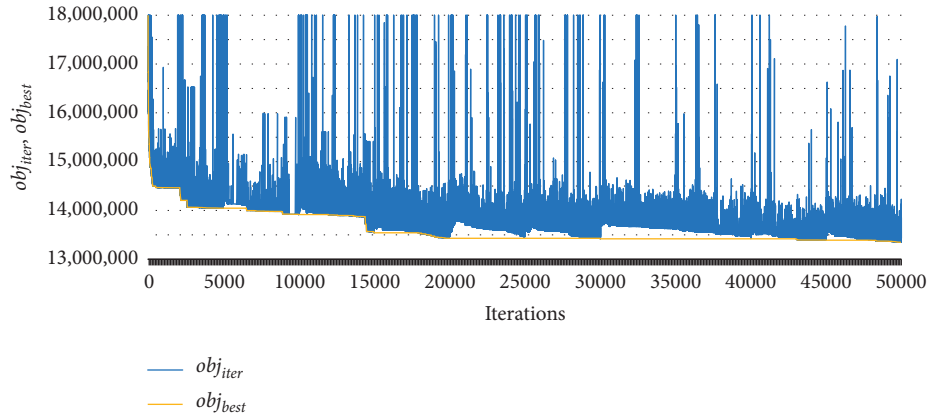

Figure 14: The variation of the objective function in each iteration.

Table 5: The explanation of comparison experiments.

Solutions	Optimize TOP	Optimize PCS	Obtained from
Origin	No	No	Real-world scenario
PCS	No	Yes	MOSA algorithm without TT and TF operators
TOP	Yes	No	MOSA algorithm without PC operators
TOP-PCS	Firstly	Secondly	MOSA algorithm
PCS&TOP	Collaboratively		PCS&TOP model and MOSA algorithm

University station to Quanyun Road station) denoted as Line 4. The operation time of the network is from 5:30 a.m. to 23: 30 p.m., covering a 1080-minute time horizon with a 1-minute time slice.

The passenger demand is obtained from the automatic fare collection (AFC) system, and a working day (December 6, 2016, Tuesday) demand data is selected as the input of this study. The distribution of passengers ($PAS^i(t)$, $PRA^i(t)$, and $PRTi, i''(t)$) can be obtained from the demand data that include the entering and exiting station and time [21], and the distributions of them are shown in Appendix C.

Other related parameters are explained and listed in Appendix C. The algorithm parameters and the computation environment are the same as those in the numerical case, and the train operation plan and passenger control strategy plan are optimized by the proposed PCS&TOP model and MOSA algorithm.

5.2.2. Result Analysis. The value of the best objective function is 13,348,194 (in $\alpha_1 = 1$, $\alpha_2 = 100$, $\alpha_3 = 0.7$). Specifically, 660 trains include 579 3-unit formation trains and 81 6-unit formation trains are used on 4 lines in total and create 117,819 train operation cost. 623,293 passengers are served and create 1,537,732 minutes of platform waiting time and 40,803 minutes of entrance waiting time. The optimized train operation plan is shown in Figure 12 In Figure 12(a), the chain lines represent the headways of the trains at the origin stations, and the translucent broken lines represent the number of arrival passengers on each line. The tendency of arrival passengers and train operation are the same. Specifically, the headway is small during peak hours and it is large during off-peak periods. The same characteristic is shown in the usage of train formation in Figure 12(b). The optimized passenger control strategies on Lines 1 and 4 are shown in Figures 13(a) and 13(b), because the passenger demand is so small that we do not need control on Lines 2 and 3. The computation process used 4647 seconds (77.46 minutes) of computation time. As shown in Figure 14, the thin blue line represents the obtained value of the objective function in each iteration, and the thick yellow line represents the best value of them. The best result rapidly decreased to a small value within 200,000 iterations. As the iteration goes on, the best result is still updating and decreasing, but the variation of results in each iteration grows smaller. That represents the search area is tapering off and convergent to a stable value.

5.2.3. Result Comparison. To explain the efficiency of the proposed model and algorithm, the optimized result is compared with different solutions from different scenarios. As shown in Table 5, 5 different scenarios are introduced.

Origin: it represents the original operation plan without any passenger control strategy, which can be obtained from the real-world plan.

PCS: it represents that the passenger control strategy is optimized only, which can be obtained from MOSA algorithm without TT and TF operators based on the origin solution.

TOP: it represents that the train operation plan is optimized only, which can be obtained from the MOSA algorithm without PC operators based on the origin solution.

Table 6: Result comparison of different solutions.

Results	*obj*	*ptf*	*pte*	*toc*	Trains
Origin	22,408,097	1,801,697	0	206,064	648 (0, 648)
PCS	22,392,307	1,739,710	65,995	206,064	648 (0, 648)
TOP	13,425,586	1,595,986	0	118,296	668 (592, 76)
TOP-PCS	13,418,168	1,558,679	42,699	118,296	668 (592, 76)
PCS&TOP	13,348,194	1,537,732	40,803	117,819	660 (579, 81)

Notes: $tr\,(tr_1, tr_2)$ in "Trains"—tr represents the total number of trains, and tr_1 and tr_2 represent the number of trains in type 1 and type 2, respectively.

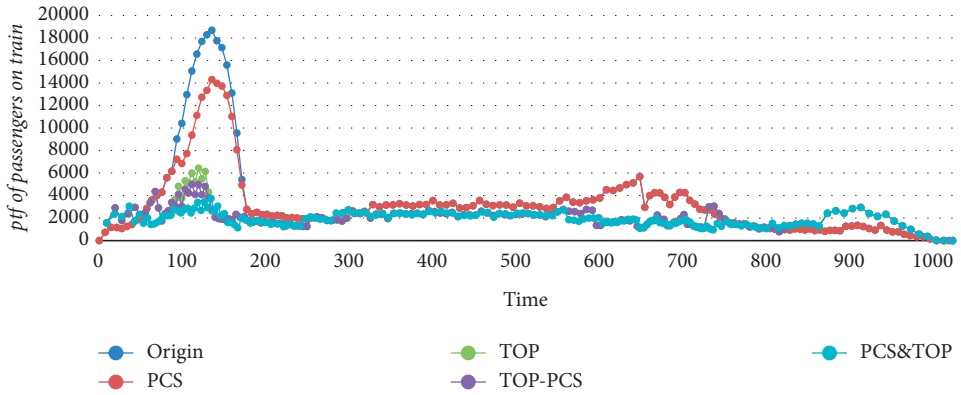

Figure 15: Platform waiting time of passengers at each train on Line 4 in different solutions.

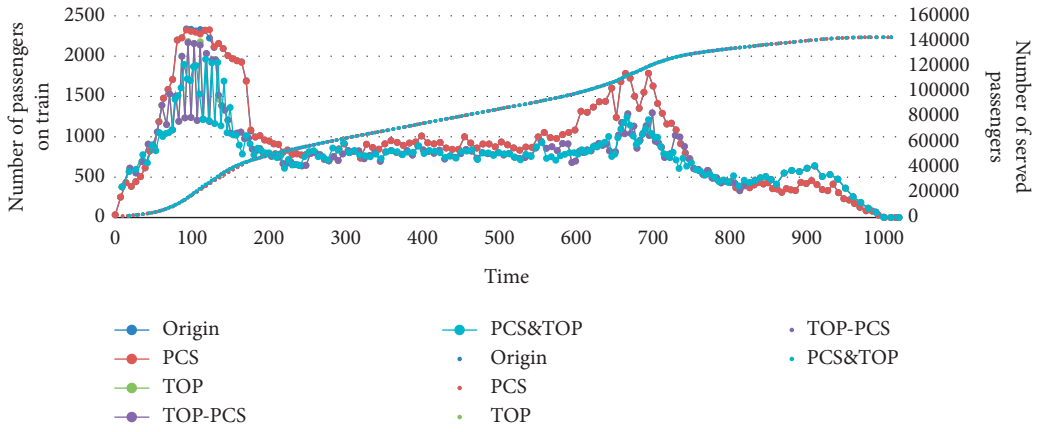

Figure 16: Number of loading passengers at each train on Line 4 in different solutions.

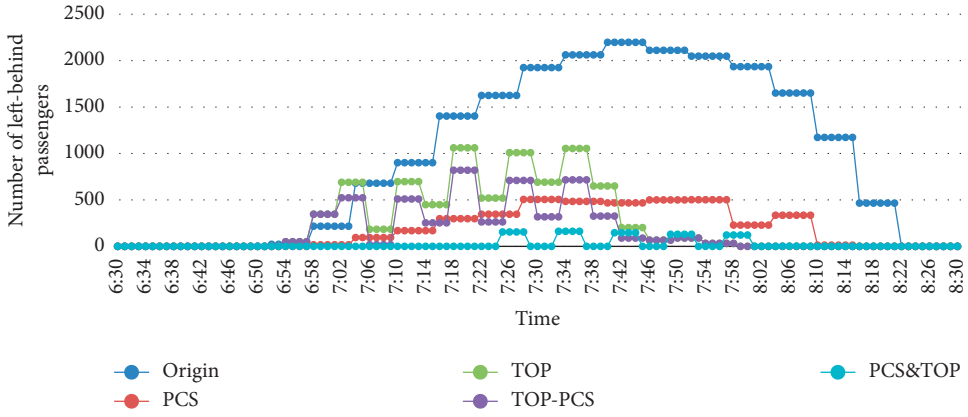

Figure 17: Number of left-behind passengers on Line 4 in different solutions.

TOP-PCS: it represents that the train operation plan and passenger control strategy are optimized, respectively, which can be obtained by optimizing the train operation plan firstly and then optimizing the passenger control strategy.

PCS&TOP: it represents the train operation plan and passenger control strategy are collaboratively optimized, which can be obtained from the proposed PCS&TOP model and MOSA algorithm.

The results that include the objective function and each part of it are shown in Table 6. Compared with the origin result, the values of the objective function are reduced by 0.07% in PCS, 40.09% in TOP, 40.12% in TOP-PCS, and 40.43% in PCS&TOP. The TOP can reduce the passenger platform waiting time, but the reduction is limited in the solution that only adjusts the train operation plan. Therefore, the TOP-PCS and PCS&TOP can reduce the passenger platform waiting time further by controlling the entering passengers. However, in the TOP-PCS solution, the passenger control strategy is optimized based on the TOP solution, in which the train operation plan may not coordinate with that. Therefore, the collaborative optimization in the PCS&TOP has a more significant effect than others. Compared with TOP-PCS solution, the objective function is reduced by 0.52% that includes 1.34% ptf, 4.44% pte, and 0.40% toc.

Due to the original train operation plan of Line 4 showing bad performance and resulting in a large number of passengers are left behind the platform, the solutions of that are worth further analysis. To explain the effect of the PCS&TOP solution, the platform waiting time of passengers, the number of loading passengers, and the number of left-behind passengers on Line 4 in different solutions are compared in detail.

As shown in Figure 15, the platform waiting time of passengers is counted in the same train on Line 4. Due to the original train operation plan is not optimized, the waiting time is very large during the morning peak hours (60–180, corresponding to 6:30–8:30) in the origin solution. Through the control of passengers in the PCS solution, the waiting time is reduced to some extent, but it is still too large. Due to the optimization of the train operation plan, the waiting time of passengers has a great reduction in the TOP solution. Based on that, the waiting time can reduce again in the TOP-PCS solution by controlling passengers at the entrance. Owing to the collaborative optimization, the PCS&TOP can further reduce the platform waiting time of passengers during peak hours.

As shown in Figure 16, the number of loading passengers of Line 4 is counted and compared. The different thick chain lines represent the number of loading passengers on each train, which shows that the number of loading passengers in the PCS&TOP solution is smaller than other solutions on most trains. The thin points with the same tendency represent the cumulative number of served passengers on each train, which shows that the cumulative number of served passengers in the PCS&TOP is similar to other solutions. It can be explained as that the passengers are served by more trains so that the loading passengers are small and the cumulative passengers are same. Due to the relative low loading rate, the passengers may have better experiences in the PCS&TOP solution than in other solutions.

As shown in Figure 17, the number of left-behind passengers on the platform of Line 4 during the morning peak hours (6:30–8:30) are counted and compared. The PCS solution has greatly reduced the number of left-behind passengers by controlling passengers at the entrance, but the

Table 7: The explanation of MOSA algorithm-related variables.

Variables	Explanation
obj_{init}	Initial result
obj_{iter}	Current result after executed
obj'_{iter}	Current result before executed
obj_{best}	Best result
s_{init}	Initial solution
s_{iter}	Current solution after executed
s'_{iter}	Current solution executed
s_{best}	Best solution
τ_{iter}	Current temperature
γ_{iter}	Current temperature reheat times
iter	Current iteration times
m	Execution operator, $m \in \text{M}$
$\rho_{l,m}$	Execution times of operator m for line l
$o_{l,m}$	Total execution times of operator m for line l
$\mu_{l,m}$	Score of operator m for line l
$\theta_{l,m}$	Weight of operator m for line l

Table 8: The explanation of MOSA algorithm-related parameters.

Parameters	Explanation	Value
τ_{start}	Start temperature	60,000
τ_{end}	End temperature	0.01
ϕ	Cooling down rate	0.9969
$\gamma_{\max}$	Maximum reheat times	10
$iter^{\text{per}}_{\max}$	Maximum number of iterations in each reheat process	5,000
$iter_{\max}$	Maximum total number of iterations	50,000
φ	Reset iteration times	100

Table 9: Dwell time and running time of the trains in the numerical case.

Station	Dwell time TW^i_l	Running time TR^i_l	
		Upward direction	Downward direction
1	1	1	—
2	1	1	1
3	1	1	1
4	1	1	1
5	1	-	1

Table 10: The train formation parameters.

Type (m)	Formation (TR^m)	Cost ($TRT^l \times TR^m$)	Capacity (Cap^m)
1	1 unit	9 minutes	150 passengers
2	2 units	18 minutes	300 passengers

Table 11: The values of numerical case train operation parameters.

Parameters	Value	Unit
TS	1	Minute
$TH_{\min}$	4	Minute
$TH_{\max}$	10	Minute
TTR_l^i	5	Minute
TRT^l	9	Minute
$NK_{l,\max}$	15	Train
RS_l	5	Vehicle
$TT^{i,i'}$	2	Minute
α_1	1	—
α_2	100	—
α_3	0.7	—

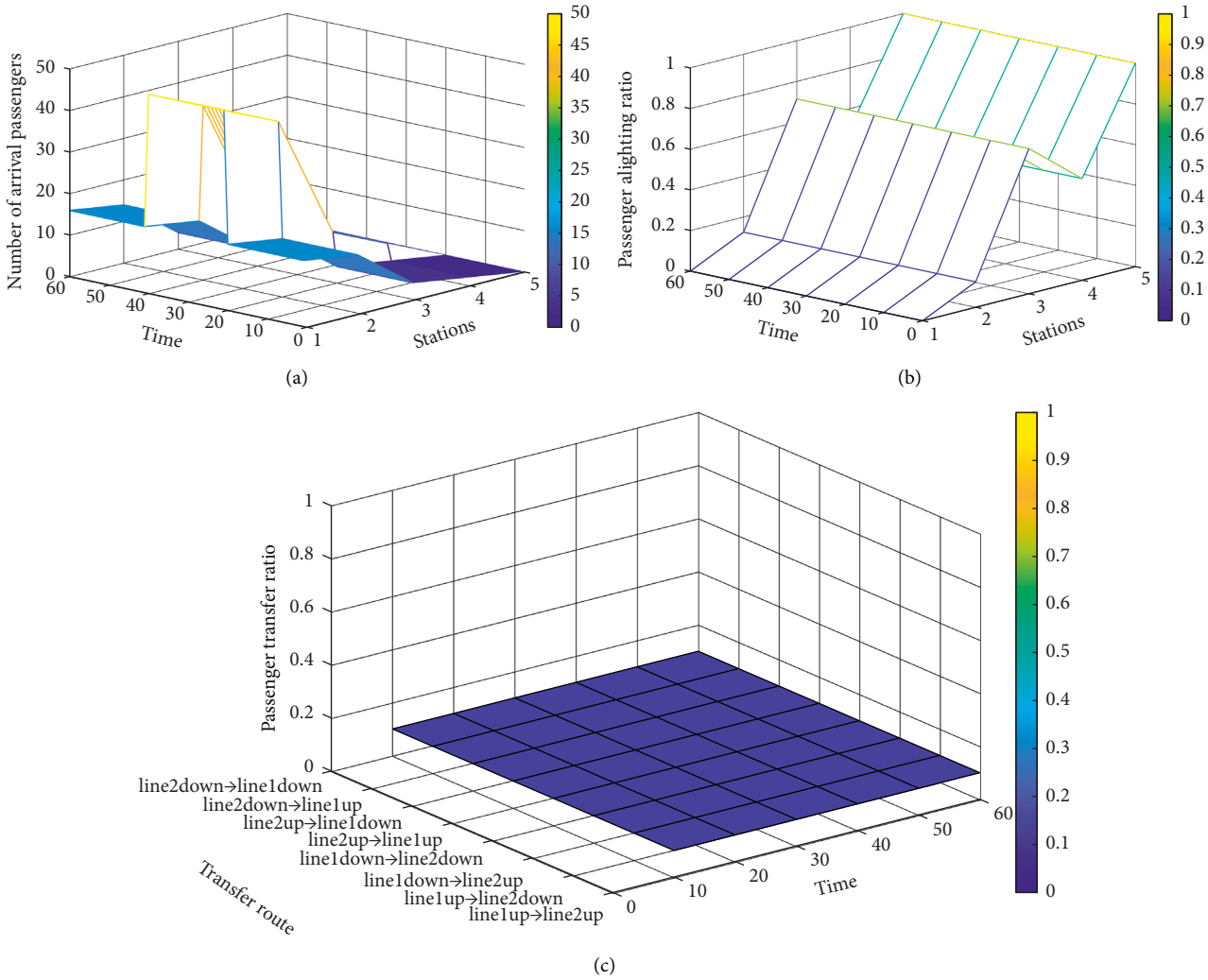

Figure 18: The passenger demand distribution in numerical case. (a) $PAS^i(t)$, (b) $PRA^i(t)$, and (c) $PRT^{i,i'}(t)$.

delay of passengers is still inescapable. The TOP solution reduces the crowding on the platform by using more trains in the peak period, but the effect is limited due to the restriction of infrastructure. The TOP-PCS solution reduced the number of left-behind passengers again by adding the passenger control strategy. Owing to the collaborative optimization, the number of left-behind passengers can be further reduced to smaller than 200 in the PCS&TOP solution.

In summary, the PCS&TOP solution optimized by the PCS&TOP model and MOSA algorithm has better performance on the efficiency of train operation plan and passenger control strategy than single optimization result and respective optimization result.

Table 12: Dwell time and running time of the trains on line 1 in Shenyang Metro.

Stations	Line 1 (upward direction)			Line 2 (downward direction)		
	No	TW_l^i	TR_l^i	No	TW_l^i	TR_l^i
Shisanhao Street	1	1	1	22	1	—
Zhongyang Avenue	2	1	1	21	1	1
Qihao Street	3	1	2	20	1	1
Sihao Street	4	1	2	19	1	2
Zhangshi	5	1	2	18	1	2
Kaifa Boulevard	6	1	1	17	1	2
Yuhong Square	7	1	1	16	1	1
Yingbin Road	8	1	2	15	1	1
Zhonggong Street	9	1	1	14	1	2
Qigong Street	10	1	1	13	1	1
Baogong Street	11	1	1	12	1	1
Tiexi Square	12	1	2	11	1	1
Yunfengbei Street	13	1	2	10	1	2
Shenyang Railway Station	14	1	1	9	1	2
Taiyuanjie	15	1	2	8	1	1
Nanshichang	16	1	1	7	1	2
Qingnian Avenue	17	1	2	6	1	1
Huaiyuanmen	18	1	2	5	1	2
Zhongjie	19	1	1	4	1	2
Zhongjie East	20	1	2	3	1	1
Bangjiang Street	21	1	1	2	1	2
Liming Square	22	1	-	1	1	1

Table 13: Dwell time and running time of the trains on line 2 in Shenyang Metro.

Stations	Line 3 (upward direction)			Line 4 (downward direction)		
	No	TW_l^i	TR_l^i	No	TW_l^i	TR_l^i
Quanyun Road	1	1	1	22	1	—
Baitahe Road	2	1	2	21	1	1
21st Century Mansion	3	1	2	20	1	2
Yingpan Street	4	1	2	19	1	2
Olympic Sports Center	5	1	2	18	1	2
Wuli River	6	1	1	17	1	2
Shenyang Library	7	1	2	16	1	1
Liaoning Industrial Exhibition Hall	8	1	2	15	1	2
Qingnian Park	9	1	1	14	1	2
Qingnian Avenue	10	1	2	13	1	1
Municipal Government Square	11	1	1	12	1	2
Financial Center	12	1	1	11	1	1
Shenyangbei Railway Station	13	1	1	10	1	1
Qishan Road	14	1	1	9	1	1
Liaoning University of Traditional Chinese Medicine	15	1	1	8	1	1
Beiling Park	16	1	1	7	1	1
Xinle Ancient Ruins Museum	17	1	1	6	1	1
Beiling West	18	1	1	5	1	1
Santaizi	19	1	2	4	1	1
Shenyang Medical College	20	1	2	3	1	2
Shenyang Normal University	21	1	2	2	1	2
Shenyang Aerospace University	22	1	—	1	1	2

Table 14: The train formation parameters.

Type (m)	Formation (TR^m)	Cost ($TRT^l \times TR^m$)	Capacity (Cap^m)
1	3 unit	159 minutes	720 passengers
2	6 units	318 minutes	1,440 passengers

Table 15: The values of real-world case train operation parameters.

Parameters	Value	Unit
TS	1	Minute
$TH_{\min}$	4	Minute
$TH_{\max}$	10	Minute
TTR_l^i	10	Minute
TRT^l	53	Minute
$NK_{l,\max}$	220	Train
RS_l	30	Vehicle
$TT^{i,i'}$	2	Minute
α_1	1	—
α_2	100	—
α_3	0.7	—

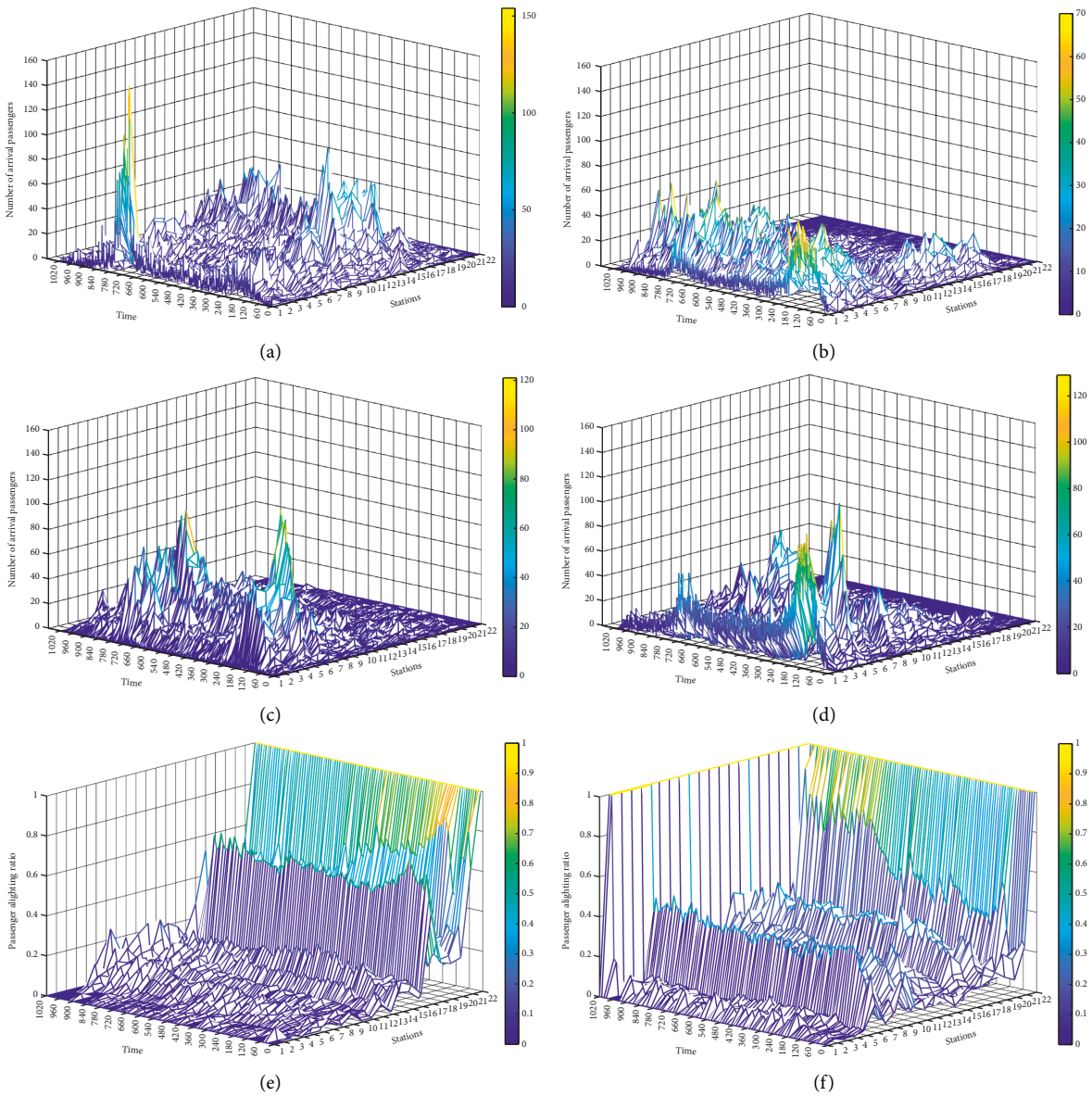

Figure 19: Continued.

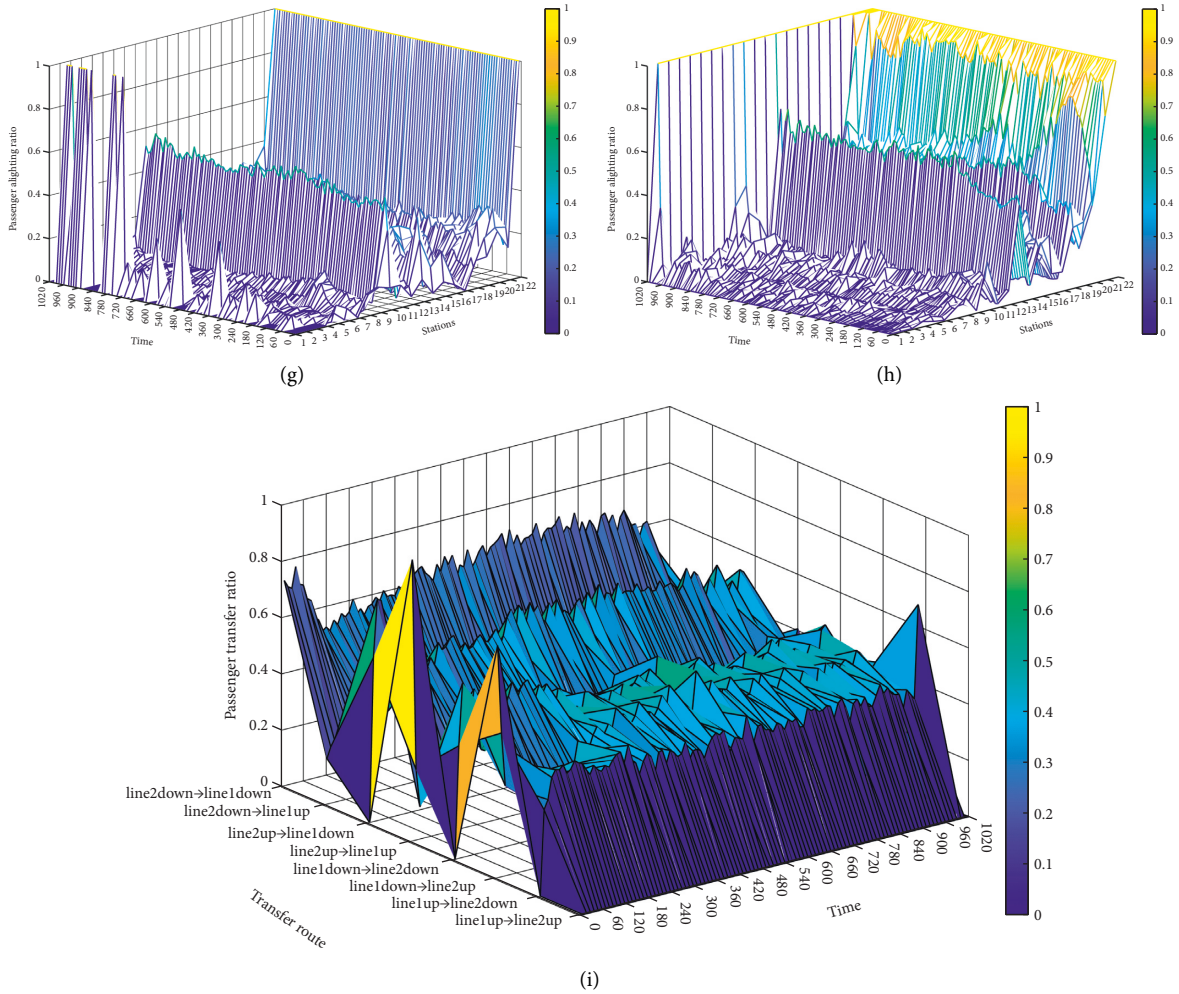

FIGURE 19: The passenger demand distribution in the real-world case. (a) $PAS^i(t)$ in Line 1, (b) $PAS^i(t)$ in Line 2, (c) $PAS^i(t)$ in Line 3, (d) $PAS^i(t)$ in Line 4, (e) $PRA^i(t)$ in Line 1, (f) $PRA^i(t)$ in Line 2, (g) $PRA^i(t)$ in Line 3, (h) $PRA^i(t)$ in Line 4, and (i) $PRT^{i,i'}(t)$.

6. Conclusion

To solve the mismatch problem between supply and demand including the oversaturated demand during peak periods and the excessed service during off-peak periods in the rail transit system, a passenger control strategy and train operation plan collaborative optimization method is proposed in this article. Specifically, the PCS&TOP model is constructed to minimize the entrance and platform waiting time of passengers and the operation cost of trains. The variable train formation plan is viewed as a decision variable to improve the flexibility of the operation plan. The turnaround of rolling stock is considered in the constraints to improve the feasibility of the optimized operation plan. The coordination of timetables on different lines is considered to improve the convenience of transfer passengers. The coordination of passenger control strategies at different stations is considered to improve the utilization of limited transport capacity. The MOSA algorithm is proposed to solve the model. To collaboratively optimize the three main decision variables, three types of corresponding execution operators are designed in the algorithm.

A numerical case that includes 2 bidirectional crossed lines is illustrated, and the stability and astringency of the model and algorithm are tested by 50 times experiments with the same parameter. The sensitivity of weight parameters in the objective function is analyzed respectively. Based on the analysis of the Pareto curve of them, the suggested range of each weight is given. The tendency of solutions with different range of weights are also analyzed to provide a reference for operators to decide.

A real-world large-scale rail transit network in China is introduced to test the performance of the proposed model and algorithm compared with the single and respective optimization solutions. Compared with the original train operation plan without passenger control, the single and respective optimization solutions have smaller objective value, but it is smallest in the collaboratively optimized solution Compared with the single and respective optimization solutions, the collaboratively optimized solution shows good performance in each aspect including the platform waiting time of passengers, number of loading passengers on the train, and number of left-behind passengers on the platform.

In future research, the method can be extended from 3 aspects: (i) The complex rail transit network with several lines and transfer stations can be applied to test the efficiency of the proposed model and algorithm; (ii) the rolling stock plan can be integrated optimized with the train timetable and train formation plan that can improve the integrity of train operation plan; and (iii) the reinforced learning approaches can be used to improve or replace the meta-heuristic algorithms to increase the efficiency of them.

Appendix

A. The Statement of the MOSA Algorithm-Related Parameters

The related variables and parameters of the MOSA algorithm are listed in Tables 7 and 8, the explanation and the suggested value of the parameters are also listed.

B. The Statement of the Numerical Case-Related Parameters

The values of train operation-related parameters in the numerical case are listed as follows. Table 9 shows the train dwell time at each station and the running time in each section. Table 10 shows the train formation parameters. Table 11 shows other train operation-related parameters.

The passenger demand distributions on each line are the same and are shown in Figure 18, which includes the number of arrived passengers $PAS^i(t)$ in Figure 18(a), passenger alighting ratio $PRA^i(t)$ in Figure 18(b), and passenger transferring ratio $PRT^{i,i'}(t)$ in Figure 18(c).

C. The Statement of the Real-World Case-Related Parameters

The values of train operation-related parameters in real-world case are listed as follows. Tables 12 and 13 show the train dwell time at each station and the running time in each section of the 4 lines. Table 14 shows the train formation parameters. Table 15 shows other train operation-related parameters in the real-world case.

The passenger demand distributions are shown in Figure 19, which includes the number of arrived passengers $PAS^i(t)$ on each line in Figures 19(a)–19(d), passenger alighting ratio $PRA^i(t)$ on each line in Figures 19(e)–19(h), and passenger transferring ratio $PRT^{i,i'}(t)$ in Figure 19(i).

Data Availability

The data used to support the findings of this study are available from the corresponding author upon request.

Conflicts of Interest

The authors declare that there are no conflicts of interest regarding the publication of this article.

Acknowledgments

This work was supported by the China Postdoctoral Science Foundation (Grant no. 2020M682590), the Science and Technology Innovation Program of Hunan Province (Grant no. 2021RC2009), and the Natural Science Foundation of Hunan Province of China.

References

[1] L. Meng and X. Zhou, "An integrated train service plan optimization model with variable demand: a team-based scheduling approach with dual cost information in a layered network," *Transportation Research Part B: Methodological*, vol. 125, pp. 1–28, 2019.

[2] N. Huan, E. Yao, and J. Zhang, "Demand-responsive passenger flow control strategies for metro networks considering service fairness and passengers' behavioural responses," *Transportation Research Part C: Emerging Technologies*, vol. 131, Article ID 103335, 2021.

[3] E. Hassannayebi, M. Boroun, S. Alaei Jordehi, and H. Kor, "Train schedule optimization in a high-speed railway system using a hybrid simulation and meta-model approach," *Computers & Industrial Engineering*, vol. 138, Article ID 106110, 2019.

[4] Y. Wang, D. Li, and Z. Cao, "Integrated timetable synchronization optimization with capacity constraint under time-dependent demand for a rail transit network," *Computers & Industrial Engineering*, vol. 142, Article ID 106374, 2020.

[5] P. Mo, L. Yang, Y. Wang, and J. Qi, "A flexible metro train scheduling approach to minimize energy cost and passenger waiting time," *Computers & Industrial Engineering*, vol. 132, pp. 412–432, 2019.

[6] H. Niu and M. Zhang, "An optimization to schedule train operations with phase-regular framework for intercity rail lines," *Discrete Dynamics in Nature and Society*, vol. 2012, pp. 1–13, 2012.

[7] Z. Cao, A. Ceder, D. Li, and S. Zhang, "Robust and optimized urban rail timetabling using a marshaling plan and skip-stop operation," *Transportmetrica: Transportation Science*, vol. 16, no. 3, pp. 1217–1249, 2020.

[8] P. Mo, A. D'Ariano, L. Yang, L. P. Veelenturf, and Z. Gao, "An exact method for the integrated optimization of subway lines operation strategies with asymmetric passenger demand and operating costs," *Transportation Research Part B: Methodological*, vol. 149, pp. 283–321, 2021.

[9] Y. Wang, Z. Liao, T. Tang, and B. Ning, "Train scheduling and circulation planning in urban rail transit lines," *Control Engineering Practice*, vol. 61, pp. 112–123, 2017.

[10] D. Wang, A. D'Ariano, J. Zhao, Q. Zhong, and Q. Peng, "Integrated rolling stock deadhead routing and timetabling in urban rail transit lines," *European Journal of Operational Research*, vol. 298, no. 2, pp. 526–559, 2022.

[11] X. y. Xu, J. Liu, H. y. Li, and M. Jiang, "Capacity-oriented passenger flow control under uncertain demand: algorithm development and real-world case study," *Transportation Research Part E: Logistics and Transportation Review*, vol. 87, pp. 130–148, 2016.

[12] F. Zhang, H. Yang, and W. Liu, "The Downs-Thomson Paradox with responsive transit service," *Transportation Research Part A: Policy and Practice*, vol. 70, pp. 244–263, 2014.

[13] S. Seriani and R. Fernandez, "Pedestrian traffic management of boarding and alighting in metro stations," *Transportation*

Research Part C: Emerging Technologies, vol. 53, pp. 76–92, 2015.

[14] F. Meng, L. Yang, Y. Wei, S. Li, Z. Gao, and J. Shi, "Collaborative passenger flow control on an oversaturated metro line: a path choice approach," *Transportation Business: Transport Dynamics*, vol. 8, no. 1, pp. 376–404, 2020.

[15] X. Xu, H. Li, J. Liu, B. Ran, and L. Qin, "Passenger flow control with multi-station coordination in subway networks: algorithm development and real-world case study," *Transportation Business: Transport Dynamics*, vol. 7, no. 1, pp. 446–472, 2019.

[16] J. Shi, L. Yang, J. Yang, F. Zhou, and Z. Gao, "Cooperative passenger flow control in an oversaturated metro network with operational risk thresholds," *Transportation Research Part C: Emerging Technologies*, vol. 107, pp. 301–336, 2019.

[17] X. Li, Y. Bai, and K. Su, "Collaborative passenger flow control of urban rail transit network considering balanced distribution of passengers," *Modern Physics Letters B*, vol. 35, no. 30, Article ID 2150461, 2021.

[18] S. Li, M. M. Dessouky, L. Yang, and Z. Gao, "Joint optimal train regulation and passenger flow control strategy for high-frequency metro lines," *Transportation Research Part B: Methodological*, vol. 99, pp. 113–137, 2017.

[19] R. Liu, S. Li, and L. Yang, "Collaborative optimization for metro train scheduling and train connections combined with passenger flow control strategy," *Omega*, vol. 90, Article ID 101990, 2020.

[20] J. Zhang, "Agent-based optimizing match between passenger demand and service supply for urban rail transit network with NetLogo," *IEEE Access*, vol. 9, pp. 32064–32080, 2021.

[21] Z. Han, B. Han, D. Li, S. Ning, R. Yang, and Y. Yin, "Train timetabling in rail transit network under uncertain and dynamic demand using advanced and adaptive NSGA-II," *Transportation Research Part B: Methodological*, vol. 154, pp. 65–99, 2021.

[22] Y. Yin, D. Li, N. Bešinović, and Z. Cao, "Hybrid demand-driven and cyclic timetabling considering rolling stock circulation for a bidirectional railway line," *Computer-Aided Civil and Infrastructure Engineering*, vol. 34, no. 2, pp. 164–187, 2019.

[23] Z. Jiang, W. Fan, W. Liu, B. Zhu, and J. Gu, "Reinforcement learning approach for coordinated passenger inflow control of urban rail transit in peak hours," *Transportation Research Part C: Emerging Technologies*, vol. 88, pp. 1–16, 2018.

[24] S. Yang, F. Liao, J. Wu, H. J. P. Timmermans, H. Sun, and Z. Gao, "A bi-objective timetable optimization model incorporating energy allocation and passenger assignment in an energy-regenerative metro system," *Transportation Research Part B: Methodological*, vol. 133, pp. 85–113, 2020.

[25] Y. Yang, Z. Yuan, J. Chen, and M. Guo, "Assessment of osculating value method based on entropy weight to transportation energy conservation and emission reduction," *Environmental Engineering and Management Journal*, vol. 16, no. 10, pp. 2413–2423, 2017.

[26] E. Aarts, "Simulated annealing and Boltzmann machines," *Handbook of Brain Theory & Neural Networks*, MIT Press, London, UK, 1989.

[27] Y. Yang, Z. Yuan, and R. Meng, "Exploring traffic crash occurrence mechanism towards cross-area freeways via an improved data mining approach," *Journal of Transportation Engineering Part A: Systems*, vol. 148, no. 8, 2022.